Analysis of Flywheel Energy Storage Systems for Frequency Support

by

Tanner Grider

A thesis submitted to the Graduate Faculty of
Auburn University
in partial fulfillment of the
requirements for the Degree of
Master of Science

Auburn, Alabama
May 1, 2021

Approved by

Eduard Muljadi, Chair, Professor of Electrical and Computer Engineering
R. Mark Nelms, Department Chair Professor of Electrical and Computer Engineering
Mark Halpin, Alabama Power Company Professor of Electrical and Computer Engineering

Abstract

Flywheels have been used to store energy in rotation for centuries. However, they were previously not suited for storing electrical energy because of their lower operating speed. However, with AC to DC converters, the flywheel energy storage system (FESS) is no longer tied to operate at the grid frequency. FESSs have high energy density, durability, and can be cycled frequently without impacting performance. Therefore, the FESS is suitable for delivering high power and low energy content to the grid. These traits make it ideal for supporting short term frequency regulation in power systems. This thesis proposes a stepwise power reference control scheme that delivers rated power and 1-2 MW below rated power to arrest frequency droop. This stepwise power reference is paired with traditional frequency dependent control to arrest the frequency early and provide fast stabilization.

Acknowledgements

I would like to thank the member of my committee, Dr. Muljadi, Dr. Nelms, and Dr, Halpin, for all their help and guidance that they have provided me given during my time at Auburn. I would like to thank my friends, Dr. Jinho Kim and all other members of the power group for their help and encouragement.

Finally, I would like to thank my parents. Without their guidance, support, and love, I would not be who I am today.

Table of Contents

List of Tables

List of Figures

List of Abbreviations

BESS Battery Energy Storage System

ERCOT Electric Reliability Council of Texas

ESS Energy Storage System

FBC Frequency-based control

FD Frequency Droop

FESS Flywheel Energy Storage System

GSC Grid side converter

ISO Independent systems operators

LS Load Shedding

MSC Machine side converter

PI proportional-integral

PID proportional-integrator-derivative

PSH Pumped Storage Hydro

PV Photovoltaic

ROCOF rate of change of the frequency

SBC sequence-based control

SG synchronous generator

1. Introduction

1.1 Renewable energy over the past decade

Over the past few decades, the power system has seen an increased use of renewable resource power plants. The higher proportion of renewable resources has reduced carbon dioxide emissions from fossil fuel power plants. As a whole, renewables contributed an estimated 26.5% of the global energy consumption; particularly, as shown in figure 1, hydroelectric and wind power met 16.4% and 5.6% of the total power generation demand in 2018, respectively [1].

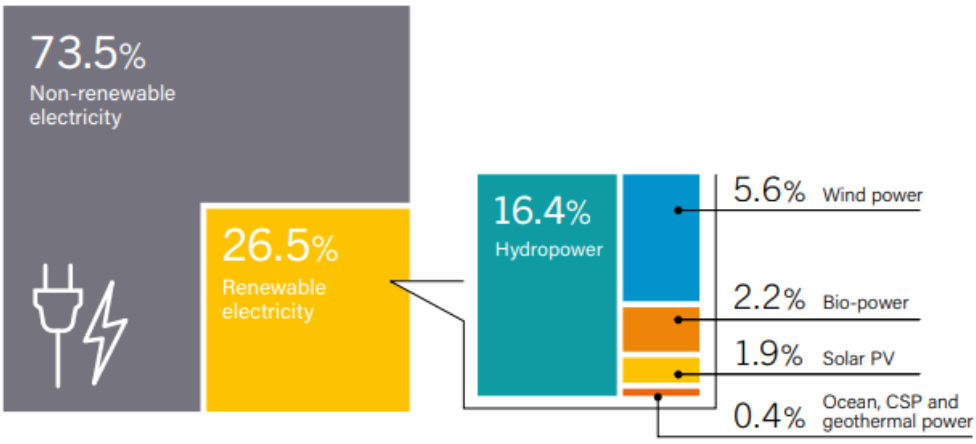

Figure 1: Renewable energy share of total production [1]

Globally, an estimated $310 billion were committed to constructing renewable power plants, compared to roughly $103 billion for fossil fuel generation plants [1]. These are partly due to the decreasing cost of renewable technology, particularly wind and solar [1]. Renewable energy investments account for nearly two-thirds of the new power generation capacity in 2017. The renewable energy sector employed approximately 10.3 million people in 2017, with solar photovoltaics being the largest employer due to solar power being the leader in new installations.

As this shift continues, and renewables meet more of the total generation, there will be a continued drop in the power system's total inertia, affecting the power system's ability to resist sudden changes.

1.2 Challenges in power systems with high penetration of renewable energy

To ensure that the power system functions and is reliable, independent systems operators (ISOs), must maintain the balance between supply and demand to keep a system frequency close to the nominal value: 60 Hz in the United States. When the supply of power matches the demand, the system frequency will stay at the nominal value. Thus, ISOs manage their power plants to follow the system demand, which continually changes throughout the day. If the system is well balanced, the system frequency will be very close to its nominal value. Otherwise, the frequency will deviate far from the rated frequency and may deteriorate the power system reliability. This issue will become increasingly challenging in the power system with high penetration levels of renewables because renewable generation resources are not controllable like those of conventional power plants. This variability and intermittency in generation is a product of weather, time of year, and the day/night cycle. Thus, renewable generation is non-dispatchable, which means increasing the penetration level of renewable into a power system will deteriorate power system stability [2]. Figure 2 shows the taxonomy of power system stability, which can be broken down into three areas: voltage stability, angle stability, and frequency stability.

Voltage stability describes the power system's ability to maintain constant bus voltage as all buses in the system [3]. Since voltage is defined as a local variable, voltage stability is affected by the reactive power balance at individual nodes. While the reactive power flow at a node remains balanced, the voltage at the node remains constant. In systems with high levels of

renewable penetration, most renewables on low voltage networks operate at unity power factor at the point of interconnection. However, this can be easily coped with by switching an operating mode of the renewables and the associated power converter at the grid interface.

Angle stability describes the system's ability to remain in synchronism when subject to disturbance, usually changes in load or generation. Increasing renewables might deteriorate this stability from varying generation levels and different ramping rates. Furthermore, the increase in renewable penetration will result in reducing synchronous rotating inertia in the system. These will make future power systems more dynamic and become vulnerable to system disturbances.

Frequency stability describes the power system’s ability to maintain the nominal frequency of the system after a disturbance in system generation or load [3]. It is affected by the balance of real power in the system. While balanced, the machines in the systems all operate at the nominal frequency. In the event of sudden supply-demand imbalance, the grid frequency will change, and the synchronous machines release their kinetic energy to resist the change in frequency. This type of response is often called the inertial response of a synchronous generator. If the system frequency decreases beyond a certain level, then the machines may be disconnected from the system to protect themselves. In this case, the power balance becomes more extreme, and may lead to a cascading event where the synchronous generators are disconnected one-by-one and will lead to an eventual blackout.

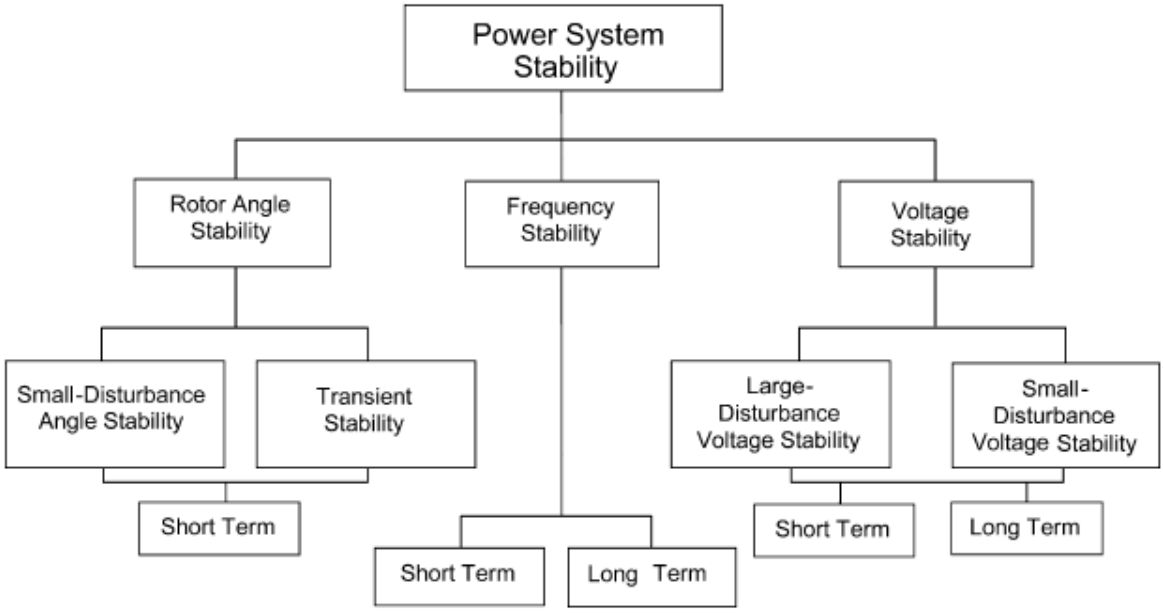

Figure 2: Power system stability breakdown [2]

1.3 Remedy-Energy Storage

Energy Storage Systems (ESS) can be used to address the variability of renewable energy generation. In this thesis, three types of ESS will be investigated: Pumped Storage Hydro (PSH), Battery Energy Storage System (BESS), and Flywheel Energy Storage System (FESS). These, and other types of energy storage systems, are broken down by their possible applications in Table 1.

PSH stores energy from the grid in the potential energy of water by pumping water from a lower elevation to a higher elevation and releasing the energy when the water flows from the upper to the lower reservoirs. It is stored in large reservoirs for use at a later time. Depending on the reservoir's size, it can supply rated power from a few hours to a few days [3]. This large amount of storage makes it ideal for providing power when wind turbine generation cuts out [3]. However, the cost of PSH systems and the location requirements make building large scale PSH systems challenging. Conventional PSH startup time is longer than other ESS, making it a poor

choice for frequency and voltage support where a fast response is necessary. Newer versions of PSH use a power converter to vary its rotational speed. Thus, it gives a quicker response and higher efficiency than the conventional PSH with a direct grid-connected synchronous generator.

BESSs use batteries to store energy in chemical bonds temporarily. The type of these bonds depends on the battery technology used. In general, batteries can provide a large storage capacity and deliver power quickly in system unbalance. However, BESSs can be costly, depending on the battery technology used, and may have lower round trip efficiency than other storage options [3]. BESSs also have decreased efficiency the more charge/discharge cycles they experience [3].

FESSs store energy in a high-speed rotating mass. A FESS consists of a variable speed electric machine (e.g., permanent magnet synchronous machine) connected to the grid via an ac-dc-ac converter to transfer electrical energy to mechanical energy and vice versa. FESSs have round-trip energy efficiency upwards of 90%, making them competitive with traditional generation [3]. This system is also low maintenance over its lifetime with fast charging and discharging times. FESSs are not capable of supplying rated power for longer durations of time (<15mins, so they are not ideal for daily load cycles or as a replacement for a downed generation). However, this quick response and high round trip efficiency make FESSs ideal for frequency and voltage support applications.

Table 1: Storage Technology and Application [3]

Applications of Storage and Possible Replacement of Conventional Electricity System Controls	Annual smoothing of loads, PV Wind, and small hydro	Smoothing weather effects: Load, PV, Wind, small Hydro	Weekly smoothing of loads and most weather variations	Daily load cycle, PV, Wind Transmission line repair	Peak load lopping, Standing Reserve, wind power smoothing, Minimization of NETA or similar trading penalties	Spinning reserve, wind power smoothing, Clouds on PV	spinning reserve, wind power smoothing of Gusts	Line or local faults. Voltage and Frequency Control. Governor Controlled generation
Full power duration	4 months	3 weeks	3 days	8 hours	2 hours	20 minutes	3 minutes	20 seconds
Conventional Capacitor								✓
Supercapacitor								✓
Superconducting Magnetic Energy Storage								✓
Flywheel					✓	✓	✓	✓
New and old Battery technologies				✓	✓	✓	✓	✓
Redox Flow Cell			✓	✓	✓	✓	✓	✓
Pump Hydro			✓	✓	✓	✓	✓	
Heat or Cold Store+ Heat Pump			✓	✓	✓	✓		
Compressed Air Energy Storage			✓	✓	✓	✓		
Large Hydro	✓	✓	✓	✓	✓	✓	✓	
Hydro Electrolysis + Fuel cell	✓	✓	✓	✓	✓	✓	✓	
Biomass	✓	✓	✓	✓	✓			

1.4 Techniques for Frequency Stability

Traditionally, frequency stability has been the responsibility of the utilities serving the regional grids. Most utilities were a vertically integrated company. Thus, the same company owns the generation, transmission, and distribution systems. Dispatchable generating units are used to adjust generation to maintain the grid frequency for any changes in the power system balance. As the grid has become more deregulated, frequency regulation, separate from the utility and independent power supplier, may be supplied as ancillary services to the grid based on the reliability market.

For the frequency to stabilize, the real power of the system must be balanced. One technique to accomplish this balance is known as Load Shedding (LS). In the past few years, the Load Resource has become available in some markets. Load Resource allows utility customers to sign a contract with the load aggregator to lower the price of electricity. With the Load Resource contract, loads can be disconnected when the ISO decides to deploy LS. Electric Reliability Council of Texas (ERCOT) has successfully implemented the Load Resource in Texas to support the supply-demand balance.

Conventional droop control applies a linear P-F curve to adjust the generator output power to correct the frequency. However, during events with frequency variations just outside of the dead-band, the fixed gain may bring about rapid acceleration/deceleration of the frequency, which can overshoot the nominal target value. A sectional droop control scheme is proposed with a smaller linear slope for small frequency changes just outside of the dead-band and larger slopes for larger frequency changes [4]. Figure 3 shows conventional and sectional droop control.

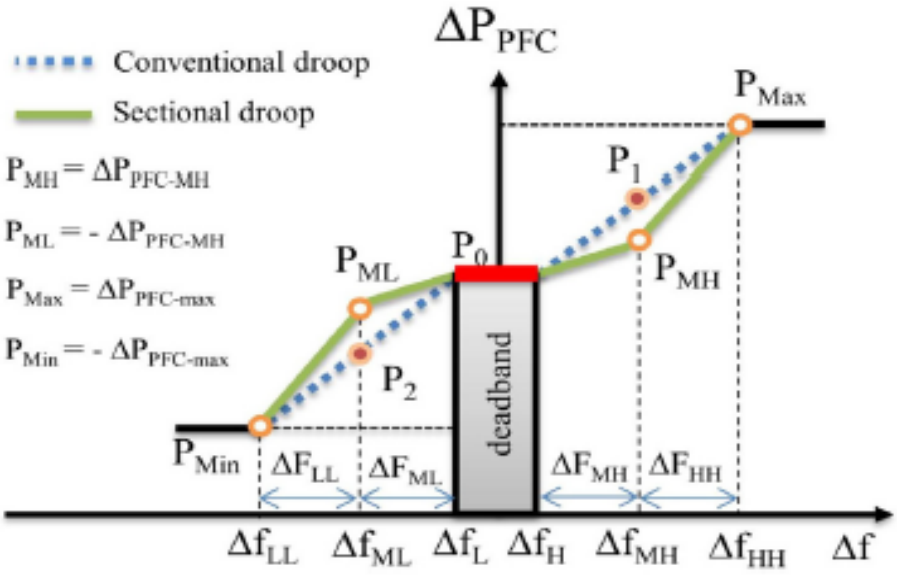

Figure 3: Conventional and Sectional Droop control [4]

1.5 Proposal

This thesis proposes a novel control method to address short term frequency drop. This method aims to address the issues that have arisen due to integrating large-scale renewable energy generation, mainly the power generation's variability. The goal of the scheme is to increase the frequency nadir, decrease the settling time, and accurately follow the reference signal.

2. Modeling

This thesis presents a dynamic model of a FESS. The model used is based on a benchmarking of Beacon's BP-400 flywheel [5]. Figure 4 shows the power characteristics of a typical FESS unit from Beacon Power. It is assumed that the FESS plant is built out of individual 100kW FESS units similar to the Beacon Power BP-400. The units can deliver 25kWh per unit or 100kW continuously for 15 minutes. The specification of the BP-400 can be found in [6]. It is assumed that the units in the presented model will operate at a maximum speed of 15 kRPM, $\omega_{max,}$ and a minimum speed of 10kRPM, ω_{min}. The moment of inertia, *J,* is also assumed to be 135 kgm^2.

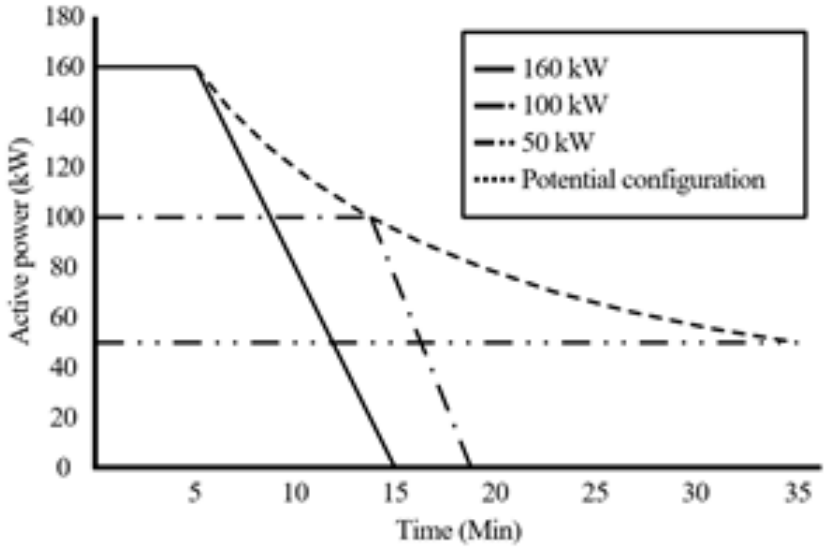

Figure 4:Output power profile of BP-400 [5]

2.1 Storing Energy in Motion

The energy stored in a flywheel, W, is proportional to the square of the flywheel's rotational speed. W can be expressed as:

$$W = \frac{1}{2} J \omega_m^2 \tag{1}$$

Where J is the moment of inertia of the flywheel, and ω_m is the speed of rotation.

The moment of inertia is determined by the size, volume, and specific density of the material used and the geometry of the flywheel. Thus, J can be optimized base on different objectives. Once the flywheel is constructed, J will remain a constant, regardless of the operating condition.

As shown in equation (1), the amount of energy stored in a flywheel is linearly proportional to J. However, it is also proportional to the square of ω_m, which incentivizes operation at higher rotational speeds such that more energy is stored.

2.2 Power and Torque

The power from the flywheel can be found from the derivative of W in (1).

$$P = \frac{dW}{dt} = \frac{1}{2}\frac{d}{dt}(J\omega_m^2) \tag{2}$$

From (2), the torque controlling the charging or discharging of energy from the flywheel is obtained by:

$$T_m = \frac{P}{\omega_m} = J\,\frac{\omega_m}{dt} \tag{3}$$

Charging energy into the flywheel is accomplished by exerting a mechanical torque and increasing rotational speed, thus storing energy in the rotating mass. Discharging energy from the flywheel can be accomplished by applying a load torque to the flywheel and reducing its rotational speed, and thus its stored energy. The instantaneous rotational speed can be found from:

$$\omega_m = \frac{1}{J}\int T_m dt \tag{4}$$

As the flywheel operates, energy will decay over time. This decay can be written as:

$$W = W_{ini} - \int P\, dt \tag{5}$$

W_{ini} is the flywheel's initial energy, and P is the power discharging from the system.

The power lost in the system can be account for through the electrical losses and the rotational losses by:

$$P_{loss} = P_{el} + P_{sp} \tag{6}$$

P_{el} and P_{sp} are the electrical and rotational losses, respectively.

2.3 Flywheel model specifications

Having assumed values for the flywheel units operating speed and moment of inertia, the maximum and minimum energy content per unit can be calculated using (1). At max rotational speed, the energy stored in the flywheel, W_{max} is 46.3kWh. At the minimum operating speed, the energy stored in the flywheel, W_{min} is 20.6 kWh. Thus, the total available energy per flywheel unit is given as the difference in the maximum and the minimum energy, 25.7 kWh. Table 2 shows the specifications of the flywheel unit under study.

Table 2: Flywheel specifications

Variable	Symbol	Value
Moment of inertia	J	135.0 kgm^2
Maximum speed	$\omega_{\max}$	15.0 kRPM
Minimum speed	$\omega_{\min}$	10.0 kRPM
Maximum energy	$W_{\max}$	46.3 kWh
Minimum energy	$W_{\min}$	20.6 kWh

3. Controls

3.1 FESS Control

Figure 5 shows a typical FESS control system. The control system is classified into two parts: the machine-side converter (MSC) controller and the grid-side converter (GSC) controller. The MSC controller controls the active power at the flywheel terminal to follow a power command, PFW-ref. PFW-ref can be determined using several techniques, as explained in the following sections.

The GSC controller controls the DC link's voltage between the MSC, the GSC, and the voltage at the terminal of the transformer. In this thesis, the FESS controls are simplified by using a current-controlled current source to inject the power from the flywheel into the system.

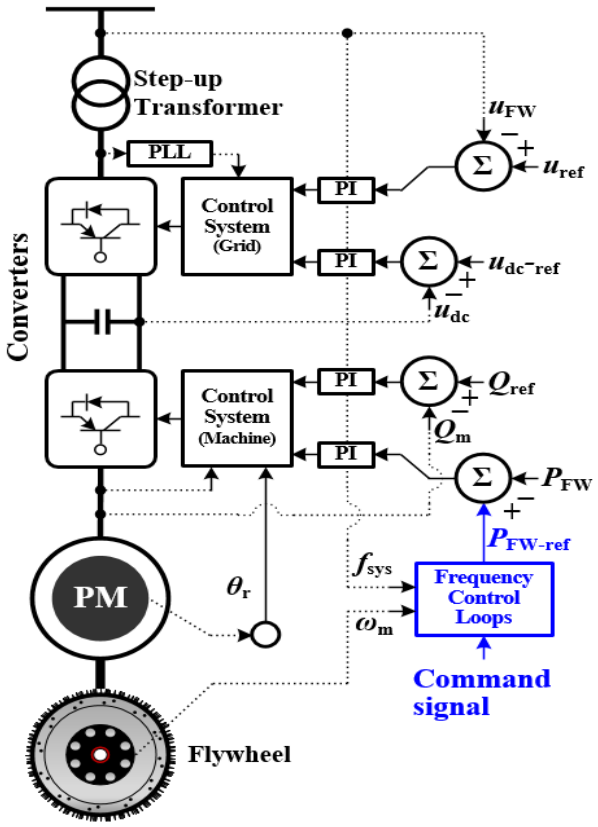

Figure 5: Typical Configuration of a FESS

3.2 Baseline

The active and reactive power of the FESS is controlled using the power converter and its controller. The controller consists of upper and lower control loops. The control loops used in this work are shown in Figure 6.

The upper loop controls the reactive power at the terminal of the FESS. To do this, first, the upper loop calculates the error between the reactive power reference, Q_{ref}, and the actual reactive power, Q_{meas}. Then, the error is processed through a proportional-integral (PI) controller to generate a quadrant-axis current reference (or reactive current reference), I_q.

The bottom loop controls the active power at the terminal of the FESS. It first determines the error between the active power reference, P_{ref}, and the measured active power, P_{meas}. Then, a PI controller is used to generate a direct-axis current reference (or active current reference), I_d.

The *dq*-currents determined in the control loops are then transformed into 3-phase current references using the Park's transformation.

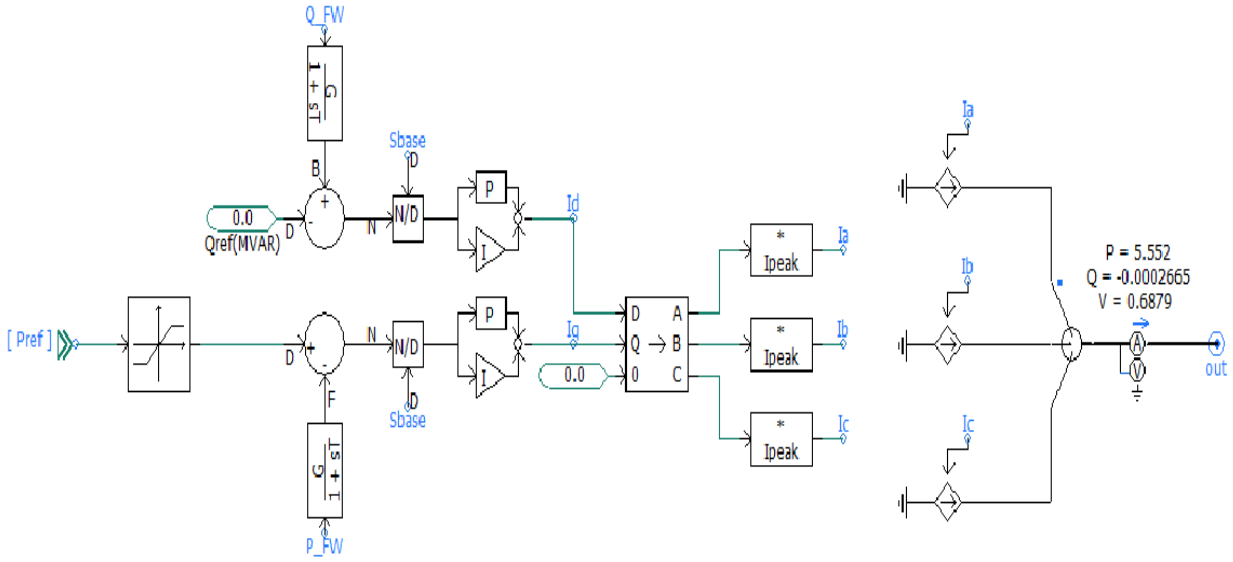

Figure 6: Converter controller of the FESS

3.3 Frequency Control of the FESS

Frequency control schemes can be realized in the FESS by determining P_{ref} according to the system frequency. There are mainly two control schemes for frequency control: frequency-based control (FBC) and sequence-based control (SBC). Both control schemes are realized through the active power control loop. The FBC determines P_{ref} of the FESS, mainly relying on the system frequency dynamics [7]– [17].

P_{ref} can be determined by processing the system frequency error through a proportional-integrator (PI) or proportional-integrator-derivative (PID) control loop in the FESS. In this scheme, the frequency control capability depends on the dynamics of the system frequency dynamics. In this scheme, an aggressive-gain setting might guarantee to arrest an initial frequency decline effectively. However, this scheme might be slow when the error is not substantial enough to lead to a quick response to arrest the system frequency.

The SBC determines P_{ref} based on the controlled system [18]–[21]. The SBC mainly includes two phases: the overproduction phase and the underproduction phase. During the overproduction phase, the controlled system supports system frequency. On the other hand, during the underproduction phase, the system restores its normal operation. Figure 5 shows an example of an SBC scheme. This scheme sets P_{ref} to a constant value in a stepwise response that is predetermined before a frequency decline is detected. Thus, it is capable of arresting the system frequency decline by providing instant power into the system. This scheme is faster at arresting the frequency decline than the FBC scheme. This quick response is desirable in systems with high penetration of renewables in order to increase the frequency nadir and secure frequency stability. However, this control strategy may cause an overcompensation (i.e.,

excessive step power increase during overproduction) and a secondary frequency dip during the underproduction phase.

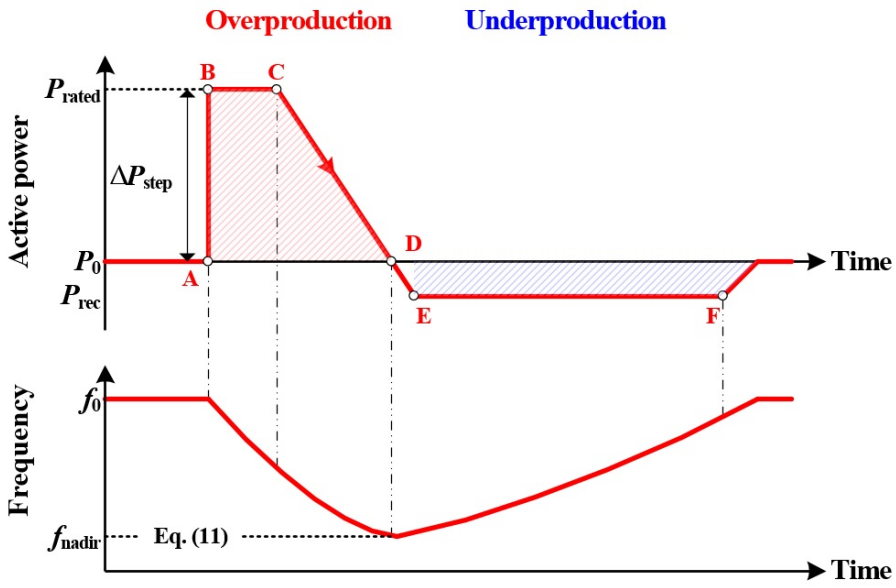

Figure 7: Example of an SBC scheme

3.4 Stepwise Control with Frequency Dependence

This control method is proposed to incorporate the fast response of a stepwise power reference with the accuracy of frequency control. This control is achieved by examining the derivative of the frequency and adjusting the power reference down once the frequency begins to return to its nominal value. Figure 6 shows the control logic that governs this operation. Figures 7-9 show the control loops in PSCAD to implement the control loop.

In Figure 8, you can see that the power reference is set to operate at point B on the switch so that when an event is detected, the reference will be set to the rated power. Once the rate of change of the frequency (ROCOF) crosses zero, the event detected signal steps the reference signal down to another predetermined value. The rate limiter block in the middle of the figure forces the reference signal to change slowly to aid the transition from the higher set point to a

lower set point. Once the frequency returns to the system's normal operating band, frequency control begins around the second set point. Once the system returns to its normal operation, the FESS is ramped down slowly to give the other generating units time to ramp their output and to save charge in the system. The speed at which FESS ramps is determined by the ramping rate of other generation on the grid.

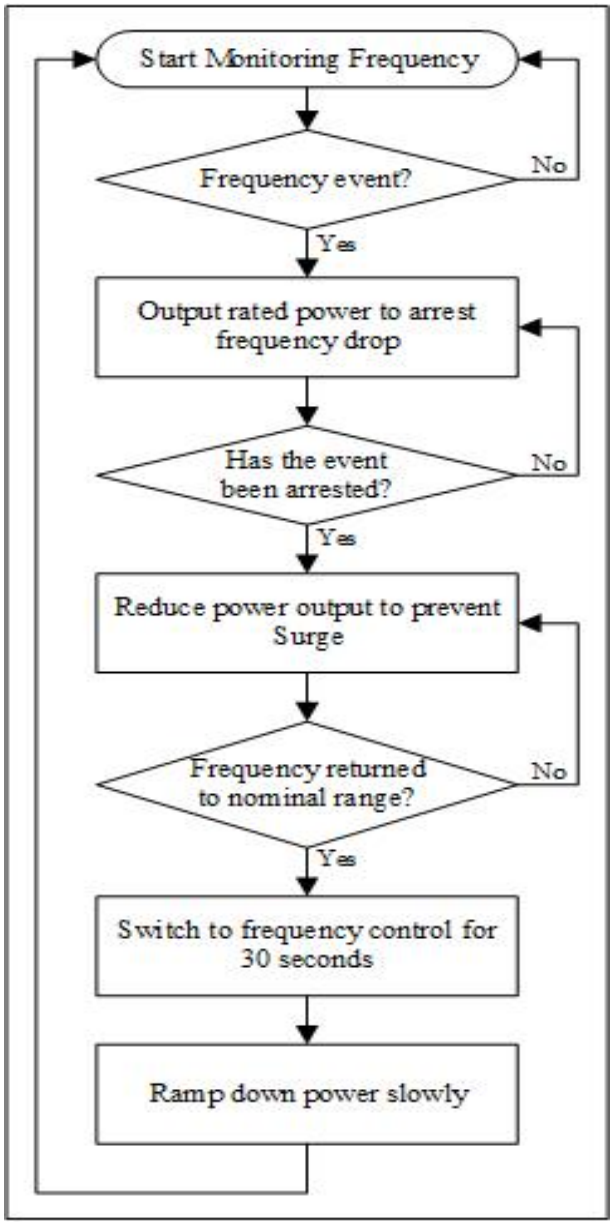

Figure 8: Propose Control loop logic.

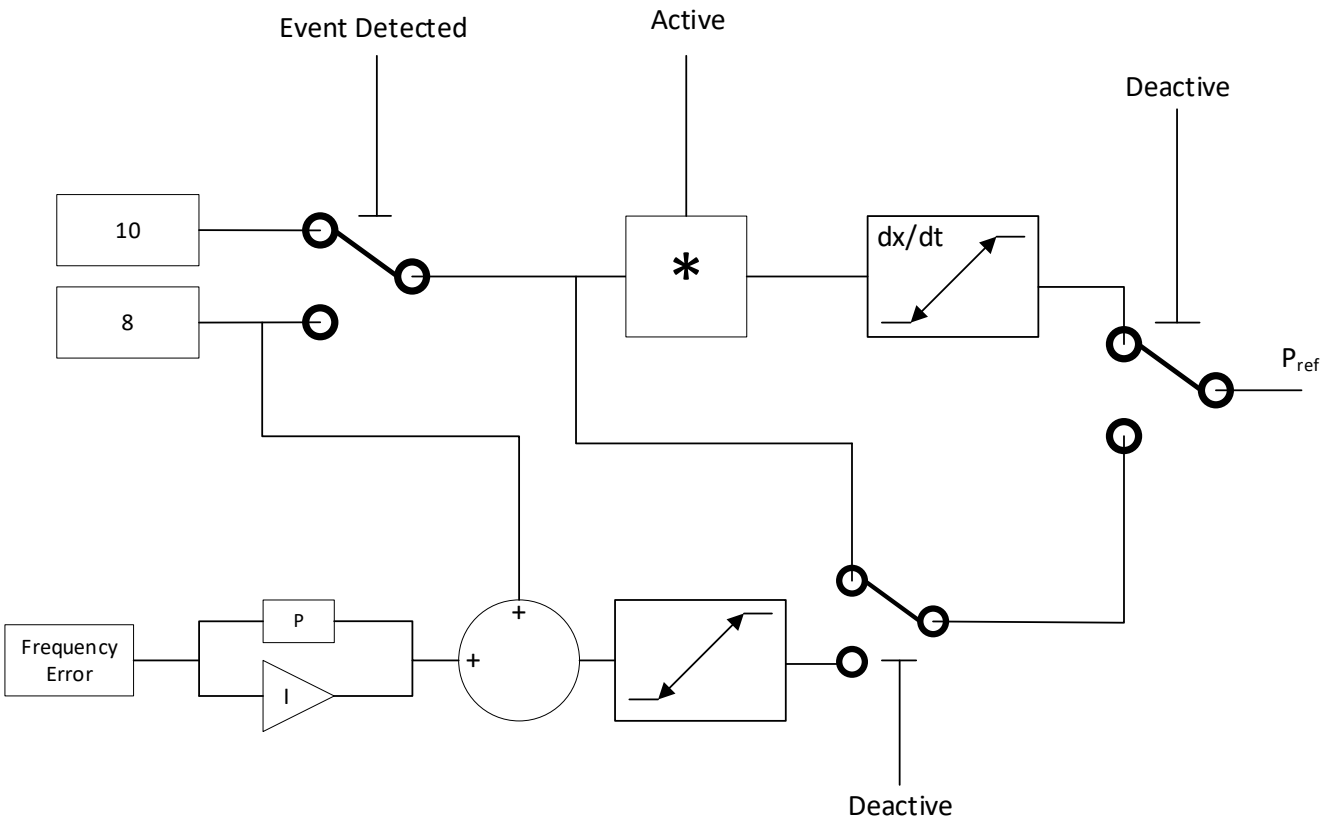

Figure 9: Main Control loop

Figure 10 governs the event-detected control signal. When the derivative of the frequency crosses zero, the signal turns on.

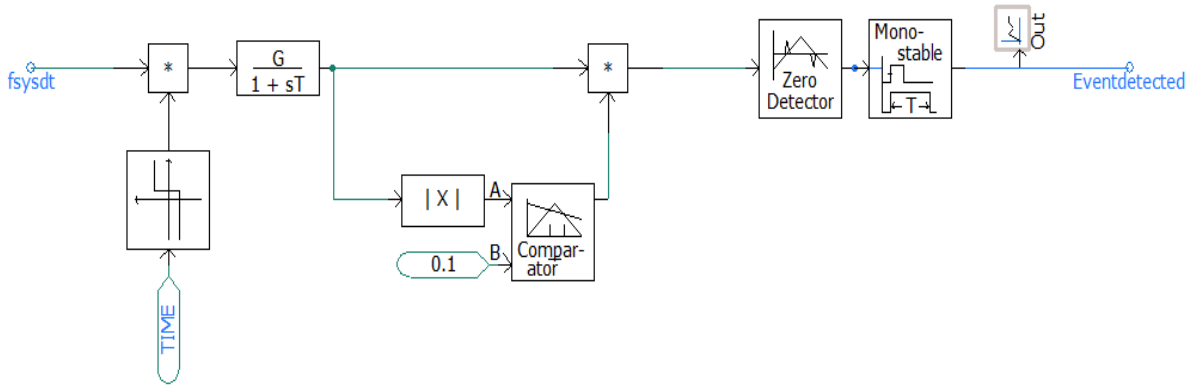

Figure 10: Event detector logic

Figure 11 controls the activate and deactivate control logic. The system is activated when the frequency drops below the determined dead-band of 0.1 of the nominal system value. The deactivate signal logic is also shown in Figure 8. It is determined by the smaller dead band of ± 0.05 of the nominal system value, the rate of change in the error, and the event detected signal.

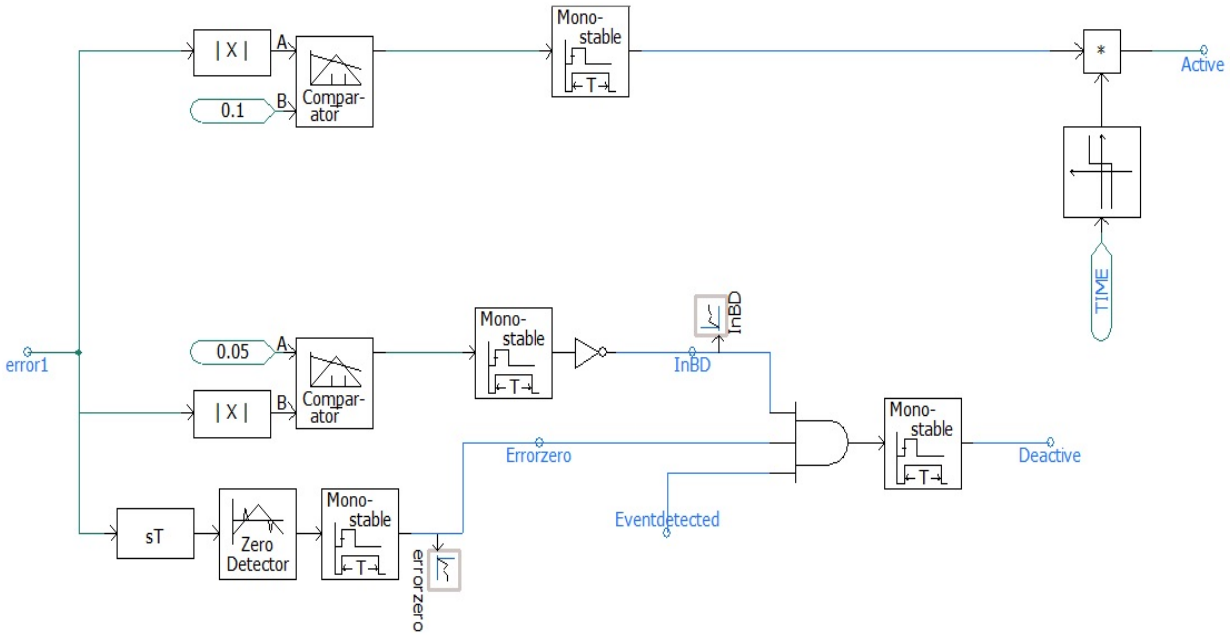

Figure 11: Deactivate logic

3.5 Voltage Control

Voltage control of the system bus can be achieved by controlling the reactive power injection into the system. The P_{ref} is set to zero, and Q_{ref} is used to calculate the error in the upper control loop. The Q_{ref} is determined by the error of the system bus voltage measured value and the desired operating value. This error is fed into a PI controller similar to the frequency control to determine the I_q current value transformed with the Park's transformation.

4. Case studies

4.1 Test system description

To verify the proposed control scheme performance, the model was simulated on the PSCAD program platform. Figure 12 shows the test system representing a scaled-down power system with renewable generation, consisting of a synchronous generator (SG), a Photovoltaic (PV) array, a FESS, and a fixed 20 MW load. The system parameters are given in Table 3.

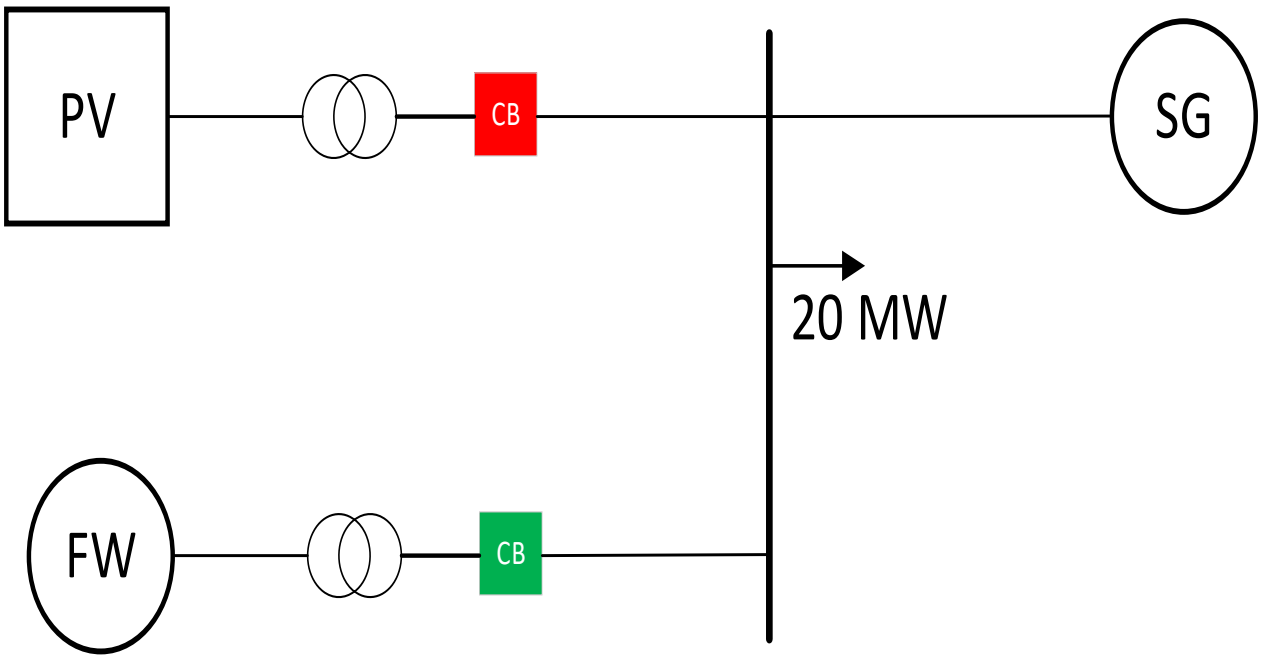

Figure 12: Test System

Table 3: System Parameters

Parameters	Flywheel	SG	PV
Rated Voltage	19 kV	19kV	19 kV
Capacity	10 MW	20 MW	10 MW
Rated Speed	1570.79 rad/s	376.992 rad/s	-
Torque [FW]	9549.297 Nm	9549.297 Nm	-

In each case, the test system complies with the load by providing electric power from the PV system and the SG. Initially, the PV system generates a fixed amount of power to the grid. To simulate frequency events, the PV system is disconnected from the grid. Thus, the system frequency declines as the load exceeds the total generation. The frequency response in the proposed scheme is monitored and compared with the baseline. As the baseline, the FESS is not activated; thus, the SG is the sole frequency response unit in the test system and is controlled using traditional droop frequency control. The baseline system will show how the synchronous generator power plant would normally react to frequency events as a benchmark to compare to the proposed control scheme which adds a Flywheel to the system. The amount of power the FESS injects into the network in each case is chosen beforehand to match the generation from the PV system. The lower step in the control scheme is chosen to be between 1 MW to 2 MW smaller than the upper step, depending on how much of the total system the PV system is supplying.

4.2 Case 1: Tripping of 5 MW of PV Generation

In this case, the PV system is operated to inject 5 MW of active power into the system, while the SG supplies the rest. After 50 seconds, the PV system is disconnected from the

network, and the frequency begins to decrease. Figure 13 (a) shows the system frequencies from the proposed scheme and the baseline. As shown in Figure 13 (a), the proposed scheme recovers the system frequency quicker than the baseline. In addition, the proposed scheme arrests the frequency nadir at a higher level than that of the baseline from 59.67 Hz to 59.86 Hz. With the proposed scheme, the system frequency nadir occurs at 1.28 seconds after the PV system was disconnected. Figure 13 (b) shows the FESS system's power reference signal and the measured power injected into the system. The FESS system follows the power reference quickly and accurately. Toward the end of both figures, it can be seen the frequency and power reference begin to decrease; this is due to the FESS system ramping down its output to save charge in the FESS once that frequency event is settled. This rate is defined by the ramp time of the system such that the system will have ample time to increase the level of output generation of the surrounding units.

Figure 13 (c) shows the active power of the synchronous generator. The response of the synchronous generator can be separated into several stages. The first stage is called the inertial response, occurring immediately as the frequency dips. Here, the kinetic energy stored in the synchronous generator is automatically released to the grid to resist the change of the rotational speed of the generator. The second stage is the governor response (primary frequency response) where the mechanical power driving the synchronous generator is adjusted following the frequency deviation from the normal frequency. Once the PV plant is tripped, the synchronous generator begins injecting its inertial response (i.e., due to a sudden change of the power angle). Afterward, the power plant governor takes action to control the synchronous generator's power level as the FESS decreases its power level from 5 MW to 4 MW. Activating the flywheel right away buys time for the governor to respond while keeping the frequency nadir above the under-

frequency setting relay. Since the change in levels is linear and relatively small, the synchronous generator can keep up with the demand without significantly changing the frequency.

Figure 13 (d) shows the mechanical torque on the FESS in per unit. With this, it can be shown that the system operates within its nameplate rating. It should be noted that the shape of the FESS torque curve is identical to the power reference curve because the torque on the system is defined by equation (3), leading it to follow the power reference.

Figure 13 (e) shows the speed of the FESS in per-unit value. The energy in the FESS is proportionally related to the square of the speed of the flywheel as in equation (1). Therefore, Figure 13 (e) represents the total charge of the FESS. Figure 13 (e) shows that the total charge of the system decreases slowly while the FESS supplies power to the grid. Since the test system is small, the FW does not lose a significant amount of its charge.

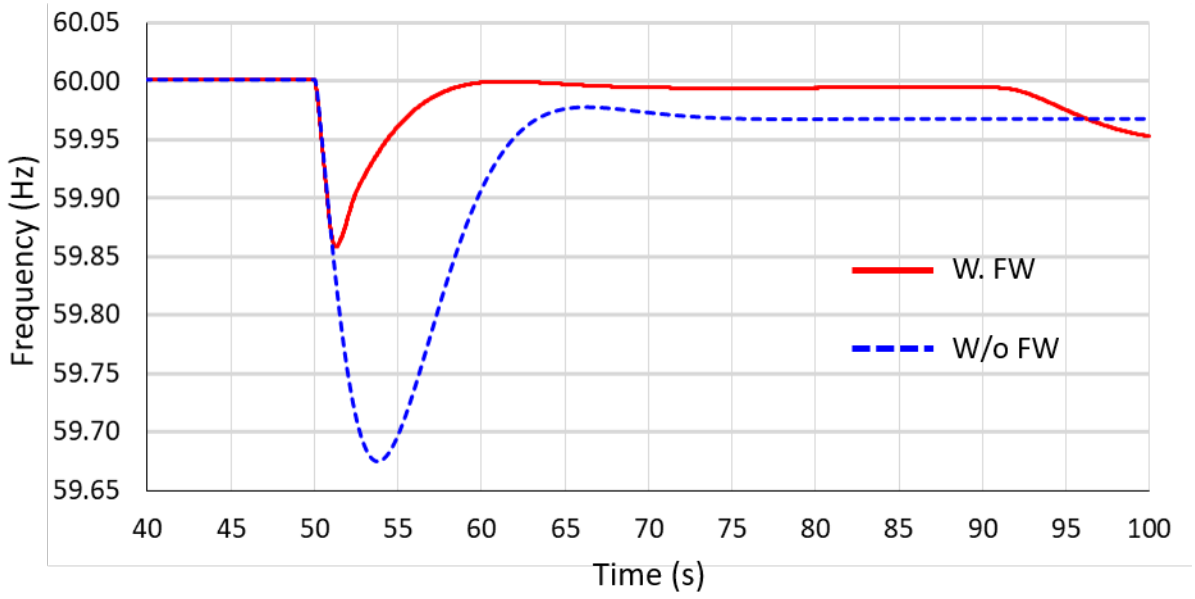

(a) System frequency

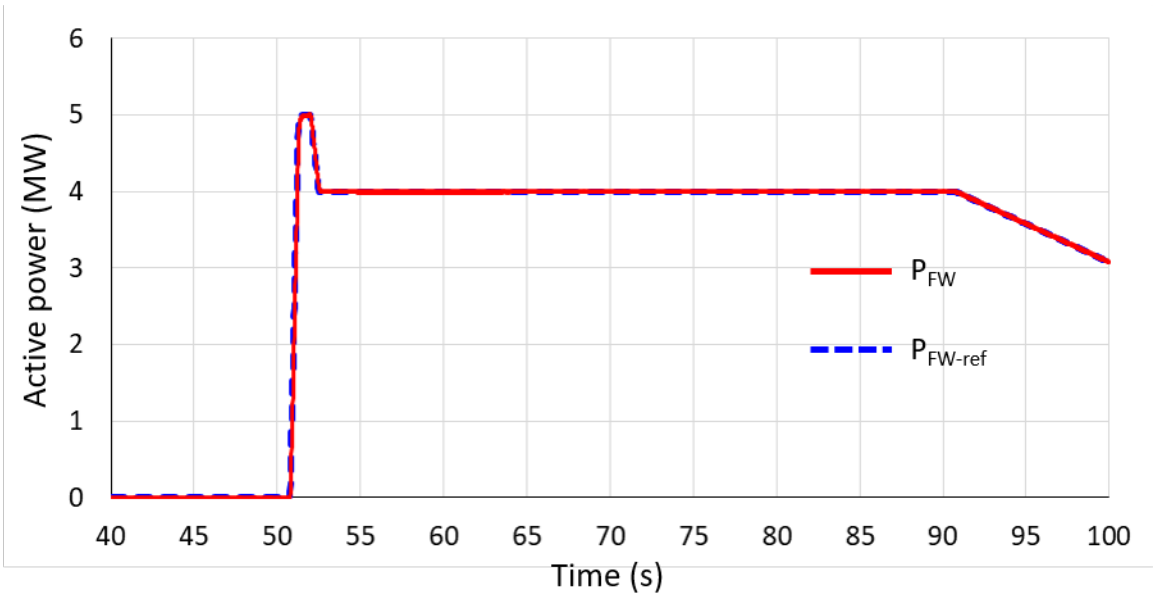

(b) Active power from the FESS

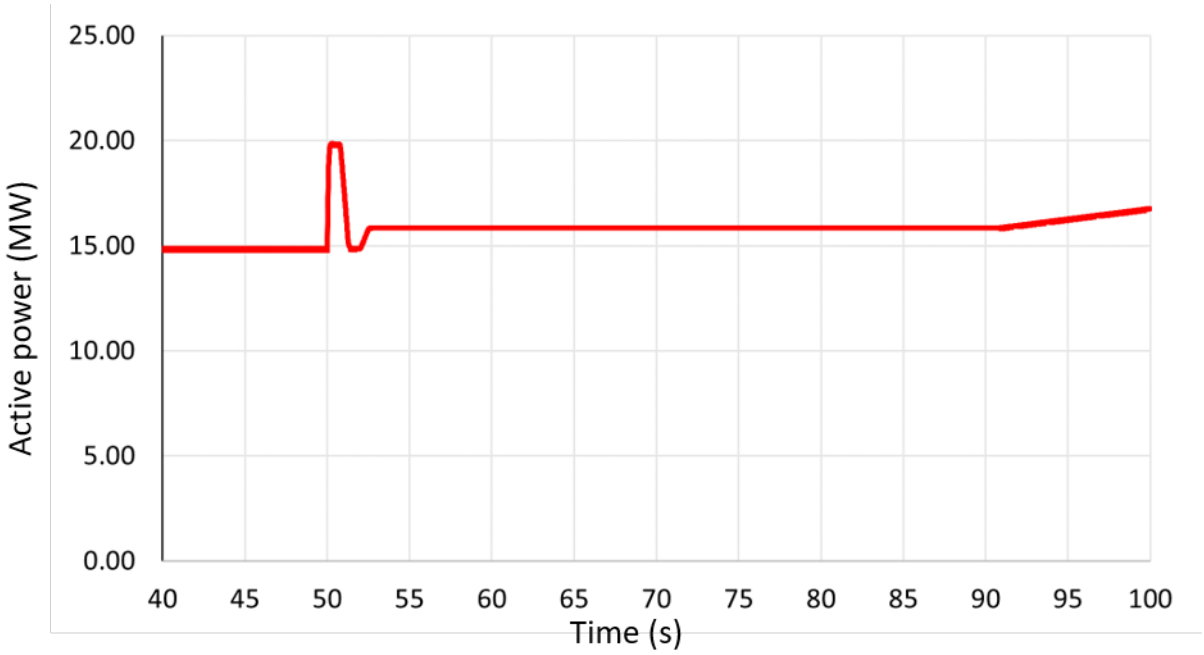

(c) Active power from the synchronous generator

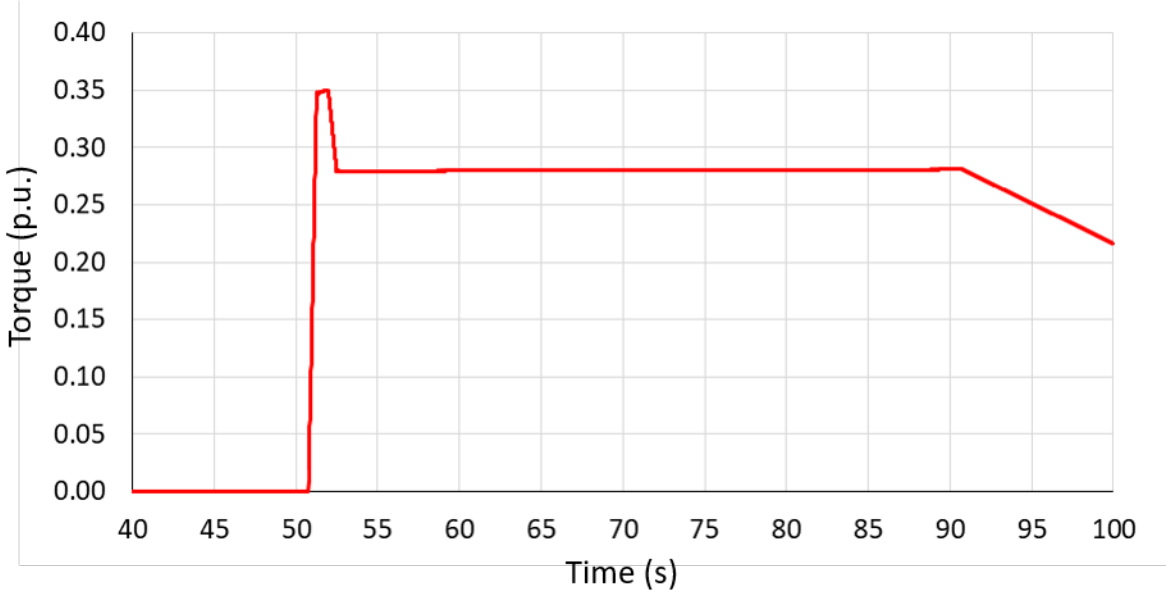

(d) Mechanical torque on the flywheel

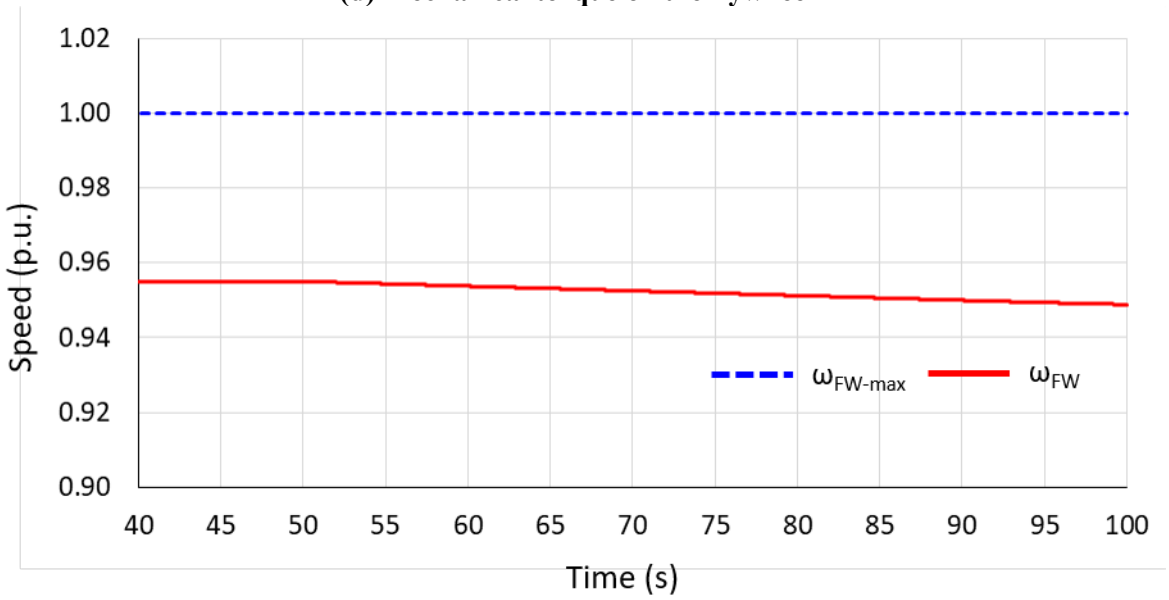

(e) Rotational speed

Figure 13: Results for case 1

4.3 Case 2: Tripping 10 MW of PV Generation

The PV system injects 10 MW of active power into the network (doubled the level of PV generation in Case 1). This case accounts for 50% of the total power needed in the system, representing a network with a very high penetration of renewable energy. The setup is the same

as in case 1, where the PV array is disconnected from the system after 50 seconds. As shown in figure 14 (a), the proposed control scheme corrects the frequency quicker than the same system while only depending on the frequency control scheme. The nadir is again increased to 59.756 Hz where before it was 59.37 Hz. The system frequency returns to within the operational dead-band after 3.5 seconds of the PV being removed from the grid. In the traditional control scheme, the system frequency does not return to the operational dead-band until 12 seconds after the PV is disconnected from the system. Also, as can be seen in Figure 14(a), the frequency swell associated with normal stepping functions is eliminated.

Figure 14 (b) shows the active power reference and the measured active power injected into the bus. As can be seen, the FESS is capable of closely following the reference signal given to it. As with the previous case, the reference signal initially supplies its upper reference set point and transition after the derivative becomes positive. After frequency control of the FESS ends, the system begins ramping its output down slowly.

Figure 14 (c) shows the active power injection of the SG. This shows that once the PV is disconnected, the SG begins supplying all of the power required by the system through the governor action. Since the PV plant is supplying 50% of the total power required, the change in active power injected by the synchronous generator is much larger and causes the large frequency drop shown in Figure 14(a).

Figure 14 (d) shows the mechanical torque on the FESS; As was true in case 1, the mechanical torque on the system follows the shape of the active power reference because of equation (3). Since this case represents the largest penetration of renewable energy, it is the most severe case of frequency drop and the most demanding of the FESS to correct. However, the mechanical torque is still less than the rated torque of the FW.

Figure 14 (e) shows the speed of the FESS for case 2; since this is the worst case for the frequency drop, it is expected that the FESS will lose the most energy to recover the system frequency in this case. While this is true because of how long the FESS is supplying power, it reminds close to fully charged.

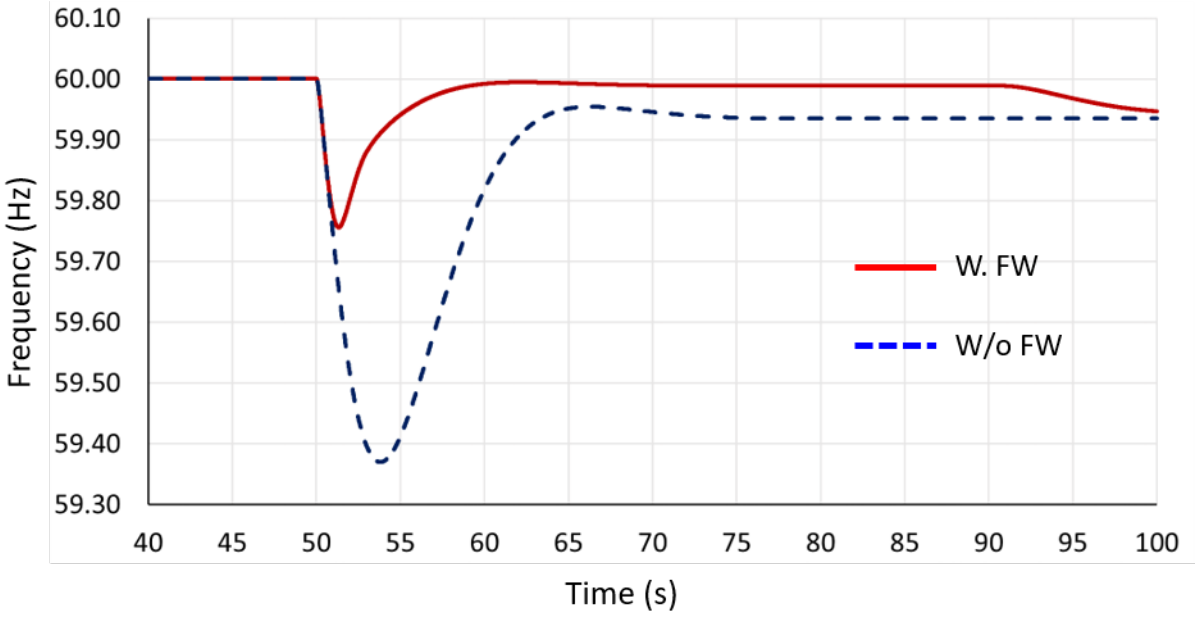

(a) System frequency

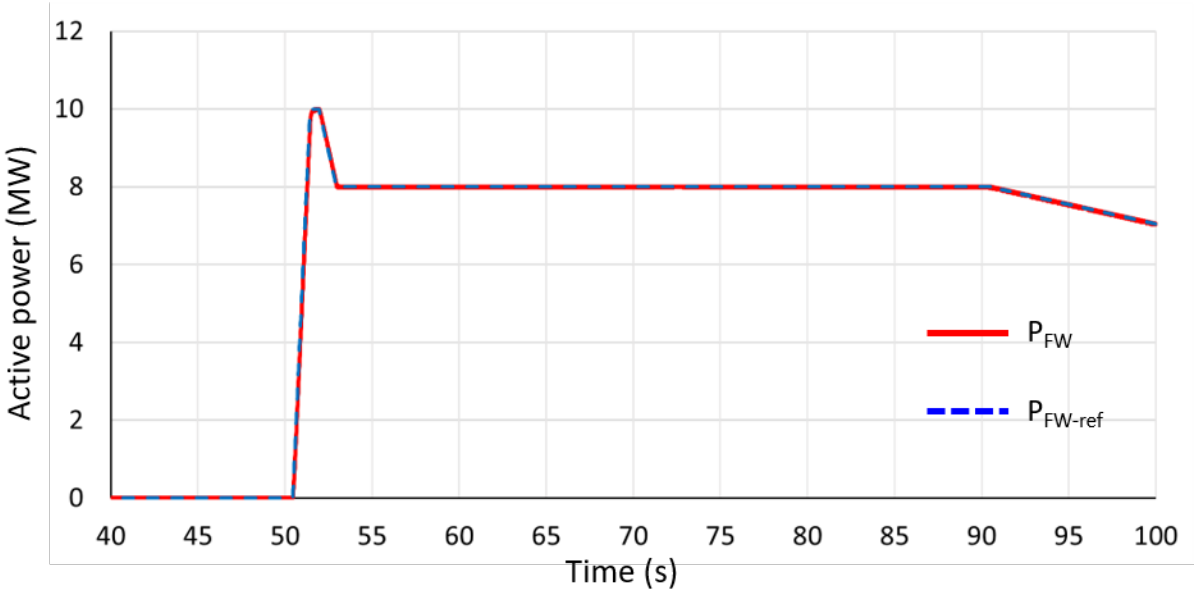

(b) Active power from the FESS

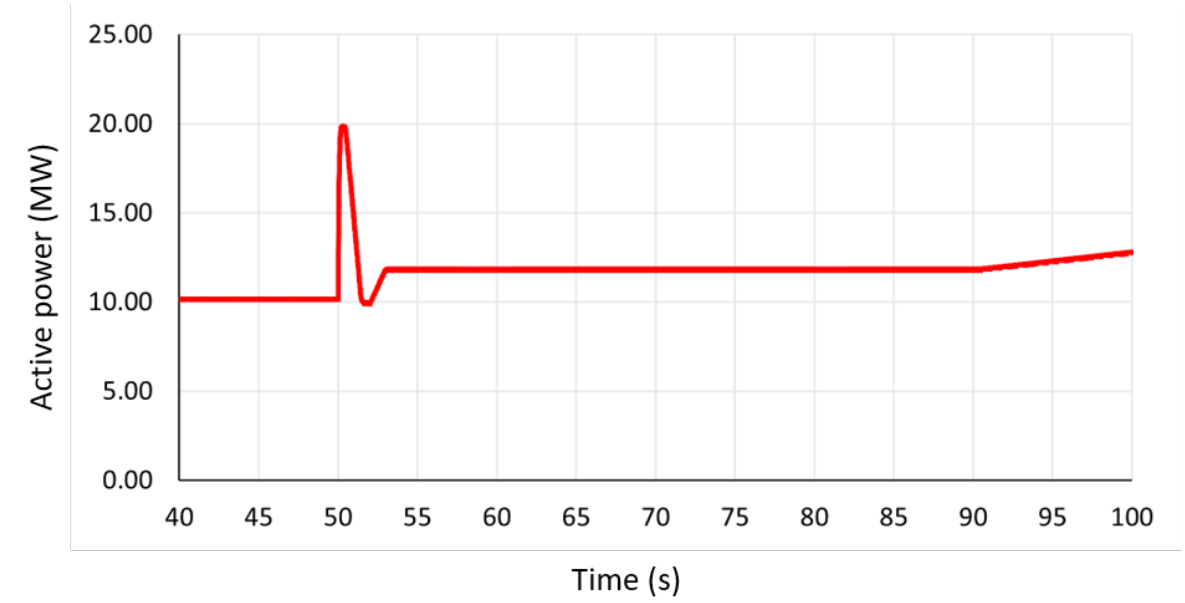

(c) Active power from the synchronous generator

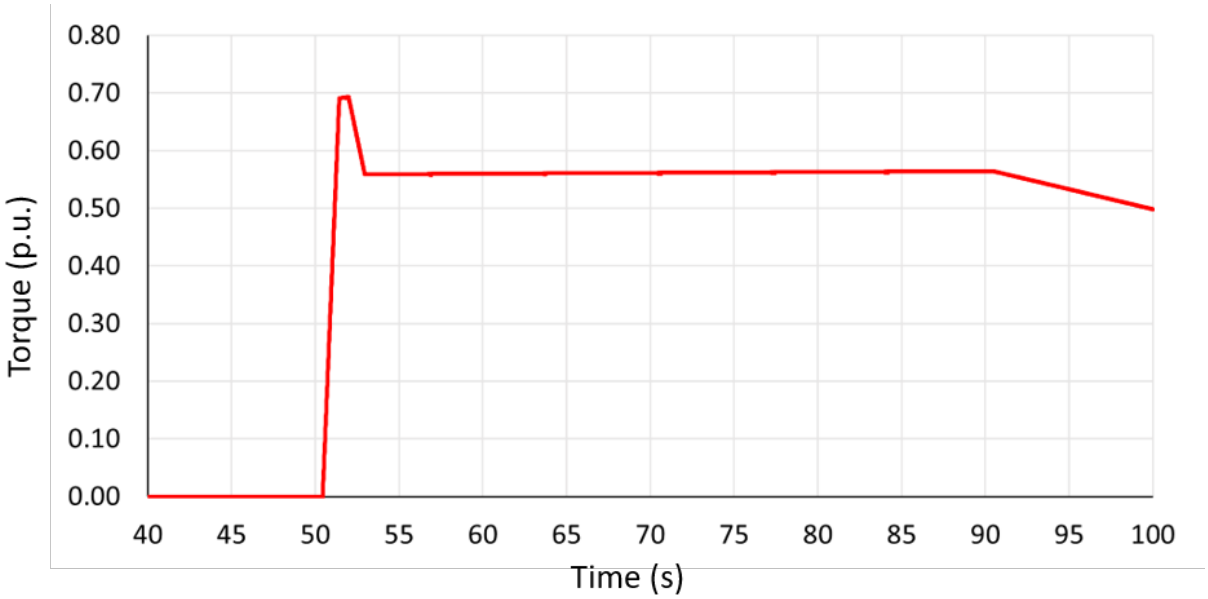

(d) Mechanical torque on the flywheel

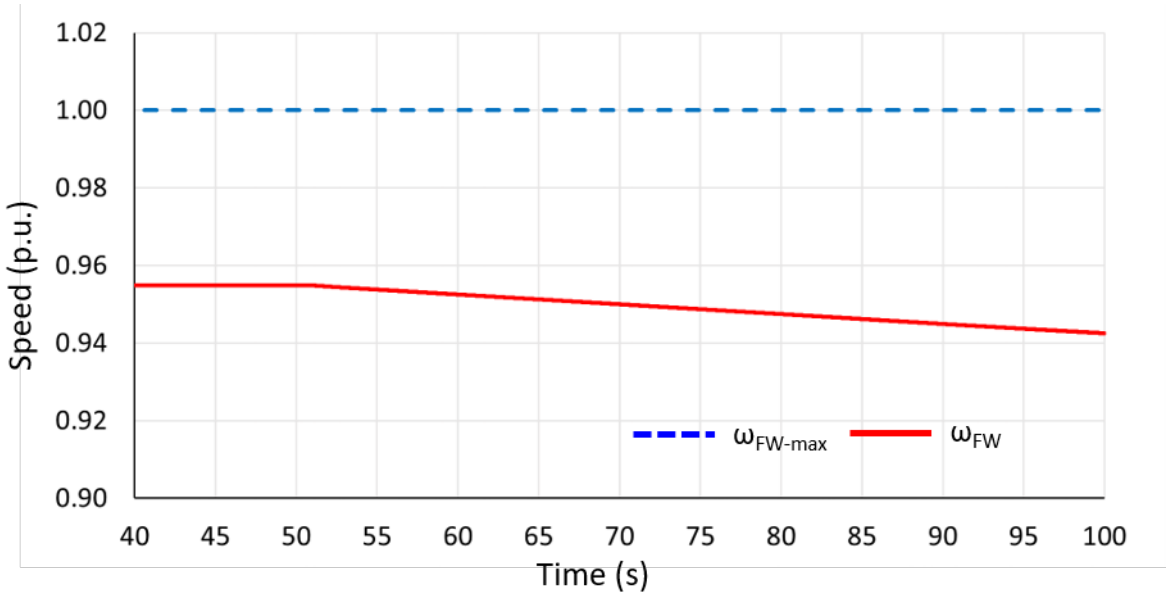

(e) Rotational speed of the flywheel
Figure 14: Case 2 results

4.4 Case 3: Tripping 2 MW of PV generation

In this case, the PV system injects 2 MW (20% of the rated power of the PV plant) of active power into the power system. As in the other cases, the PV is disconnected from the system at 50 seconds to simulate the loss of production of the PV power plant. At which point the system frequency begins to decline because of the imbalance of active power in the network. Figure 15 (a) shows the system frequency before and after the proposed control method. Since, in this case, the PV accounts for a smaller fraction of the total active power supplied, the frequency droop is shallow. This allows the system in both cases to recover quicker than either of the cases presented previously. In this case, as well the frequency nadir is increased and moved to the left, showing that the system is recovering faster than the traditional method. The frequency nadir occurs at 59.87 and 59.897, respectively. Figure 15 (b) shows the active power reference and the measured injected power by FESS system. It is shown that the FESS follows the reference signal quickly and precisely. In this case, the down ramping when Droop control

ends is steep with respect to the lower step power level. In this case, the down ramping of the FESS would need to be slower to prevent the system from activating again. This is caused in part because the synchronous generator is operating in frequency control mode, which adjusts its output slower for smaller changes in the system frequency.

Figure 15 (c) shows the active power injected into the power system by the synchronous generator. In this case, the change in power injection for the synchronous generator is small compared to the amount of power that is already being injected. Because not a lot of power is being tripped off, the frequency droop is slower than in previous cases, causing the system to react slower.

The mechanical torque on the flywheel is shown in Figure 15 (d). Its shape follows that of the power reference due to equation (3). In this case, the max torque applied to the system in only 14% of the rated torque of the machine, well within the operating limits of the flywheel.

The charge of the FESS can be seen in Figure 15 (e) since the charge is directly proportional to the square of the rotational speed of the flywheel, as seen in equation (1). As such the change in speed of the flywheel is small in this case.

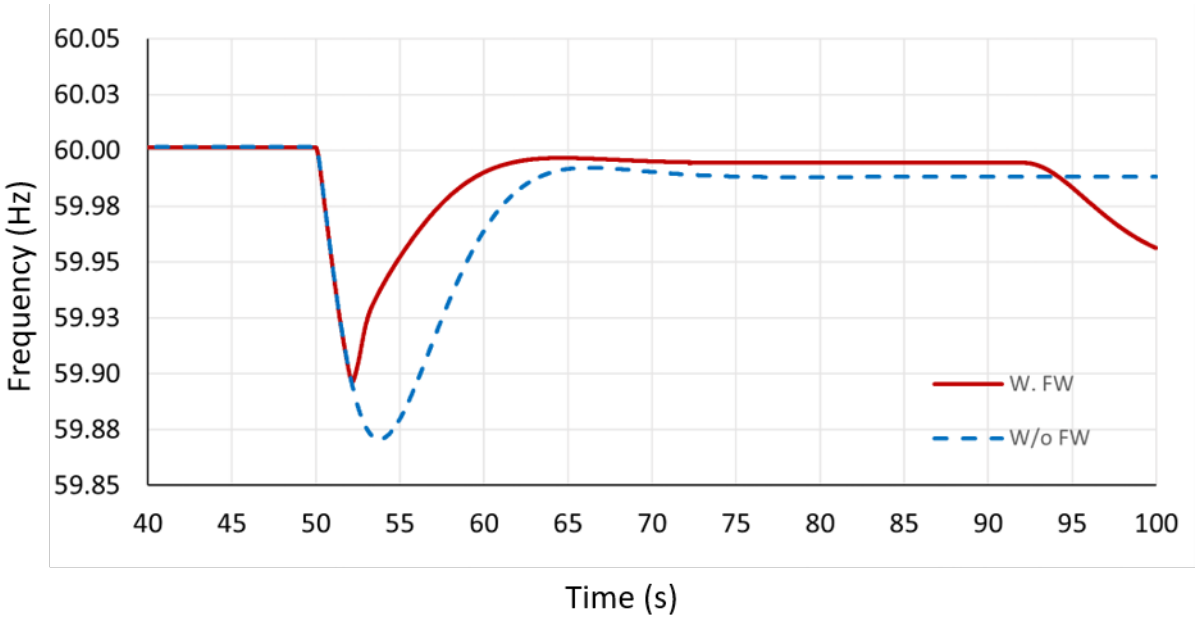

(a) System Frequency

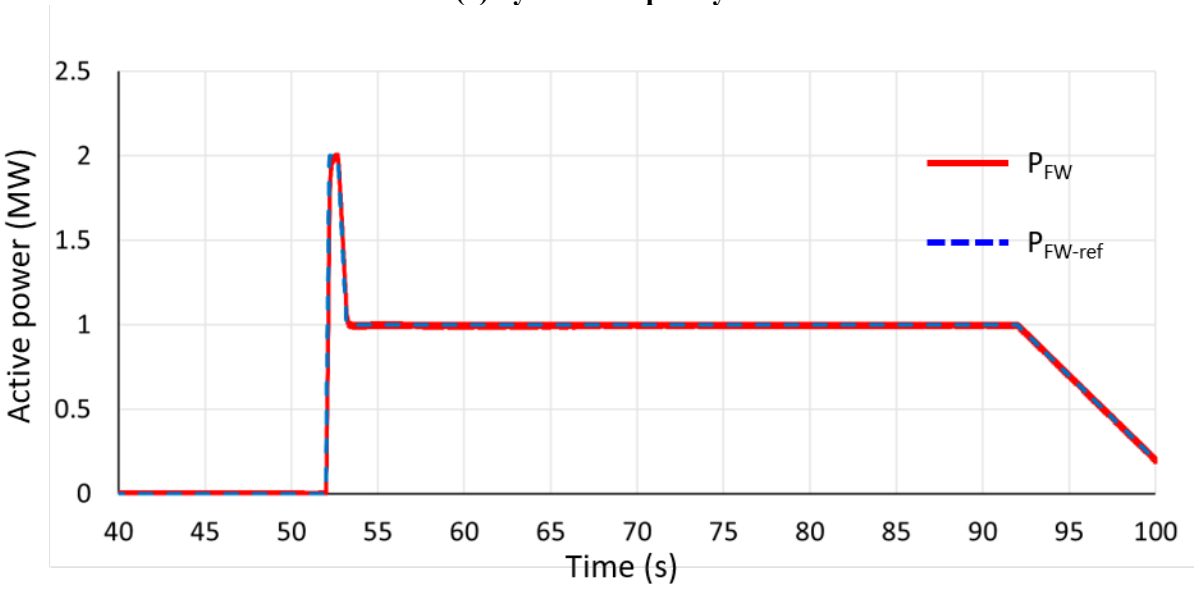

(b) Active power from the FESS

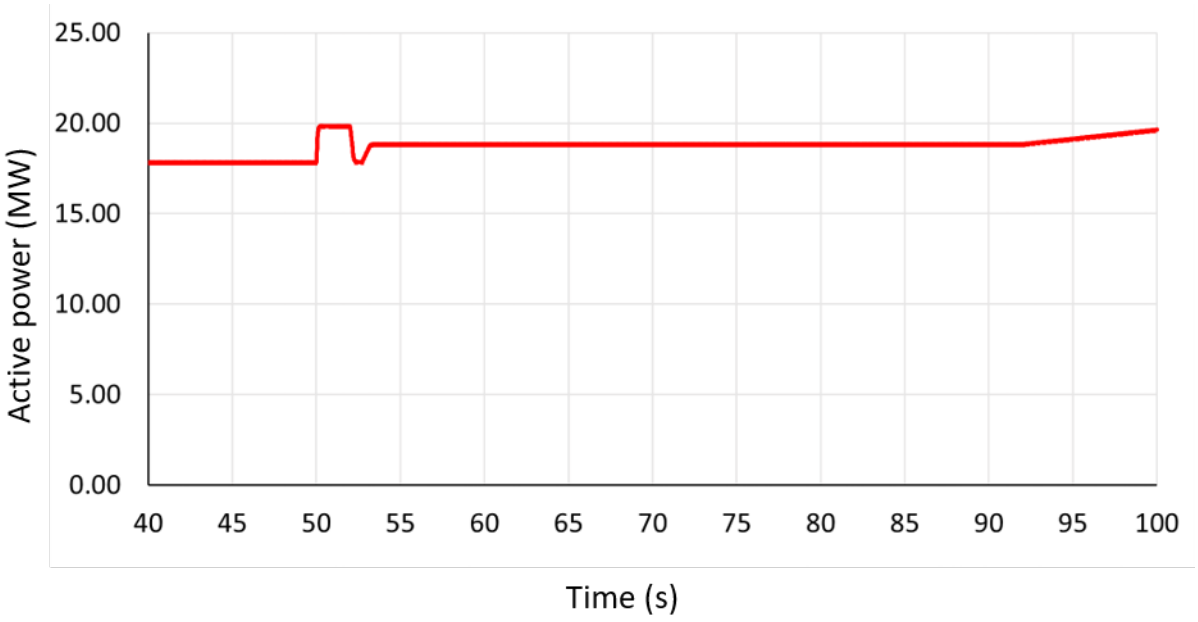

(c) Active power from the synchronous generator

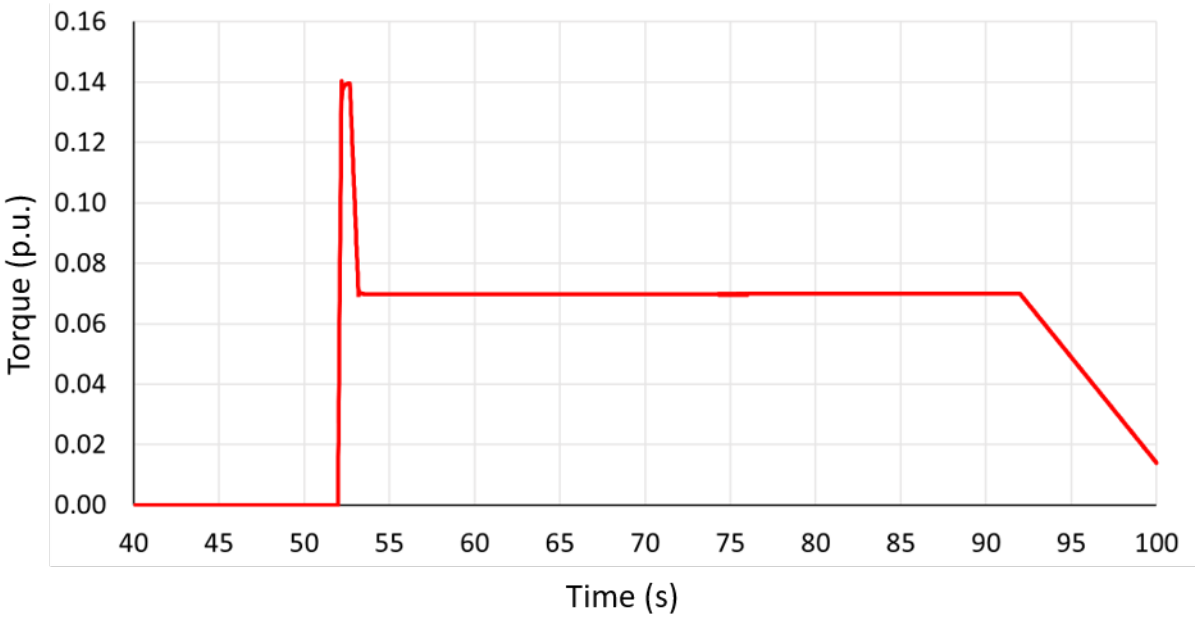

(d) Mechanical torque of the flywheel

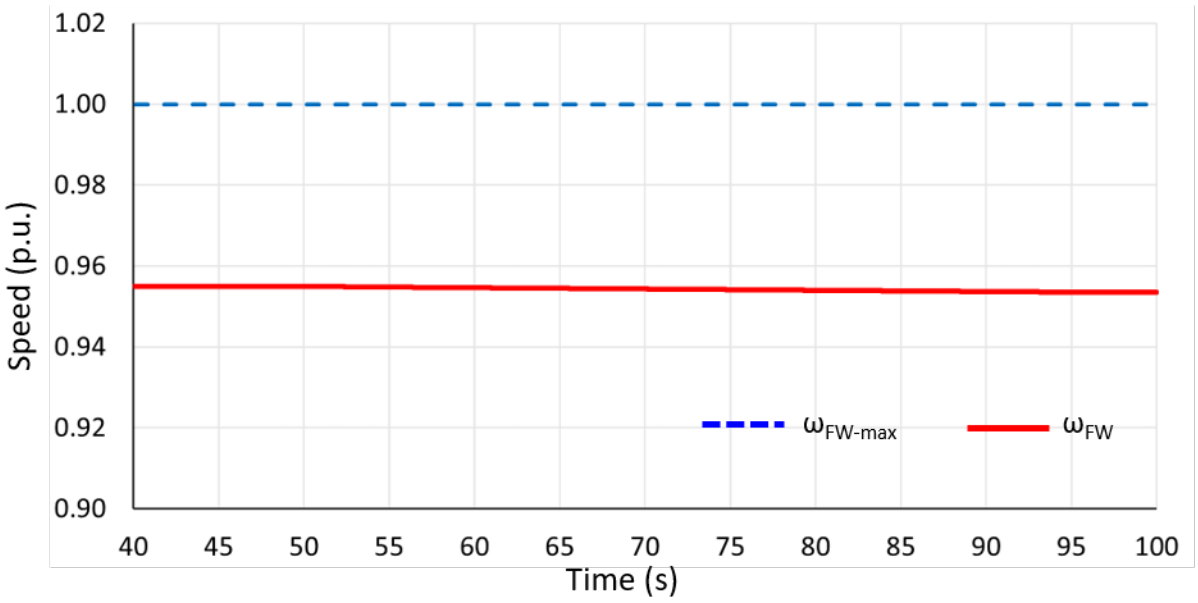

(e) Rotational speed of the flywheel
Figure 15: Results for Case 3

4.5 Case 4: Tripping 8 MW of PV generation

In this case, the PV system injects 8 MW of active power into the power system. After 50 seconds, the PV system is tripped to simulate a loss of production, and the frequency begins to decline. Figure 16 (a) shows the system frequency before and after the proposed control scheme was implemented. Without the proposed control scheme, the synchronous generator is able to arrest the frequency at 59.4798 Hz. With the proposed control scheme, the frequency was arrested at 59.7982 Hz. These occur at 3.80 seconds and 1.28 seconds after the PV system is tripped, respectively. This shows that the proposed control scheme can arrest the droop quicker than traditional control leading to a faster recovery to the nominal operating band of the system. Also seen in Figure 14(a), the frequency begins to decrease towards the end of the simulation due to the down ramping of the FESS. Figure 16 (b) shows the FESS power reference signal and the measured output of the FESS. As shown when a frequency droop is detected, the FESS

begins to output the rated power of the system. After the frequency stops decreasing, the FESS decreases its power injection to its lower step. After droop control of the FESS ends, the system begins to reduce output to save the charge in the system.

Figure 16 (c) shows the output of the synchronous generator during the frequency decline. When the droop begins the real power, injection increases to supply the load. This is the cause of the frequency droop as the synchronous generator tries to deliver that power. Once the flywheel begins injecting power, the output of the synchronous generator drops back to the level, it was at previously.

In Figure 16(d), the mechanical torque on the flywheel can be seen. In this case, the mechanical torque on the system is below its rated value, and the shape of the torque follows that of the power reference signal due to the relationship seen in equation (3).

Figure 16(e) shows the speed of the flywheel; As the FESS injects power into the grid, the flywheel slows down. The speed also represents the total charge left in the FESS because of equation (1), so as the system injects power, it will lose its charge.

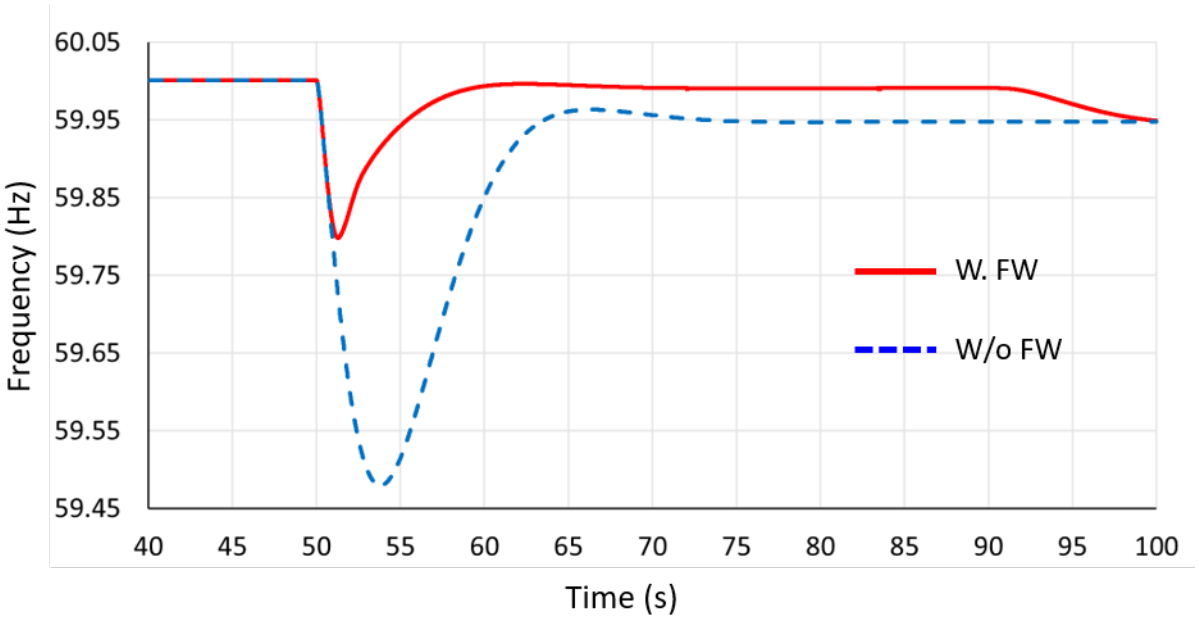

(a) System Frequency

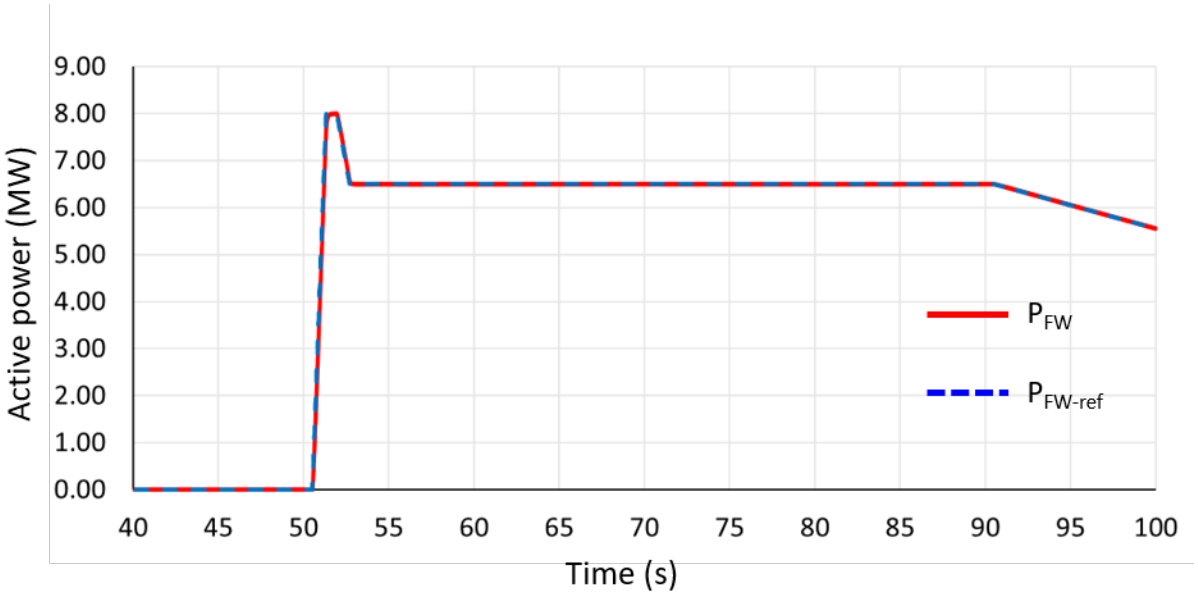

(b) Reactive power from the FESS

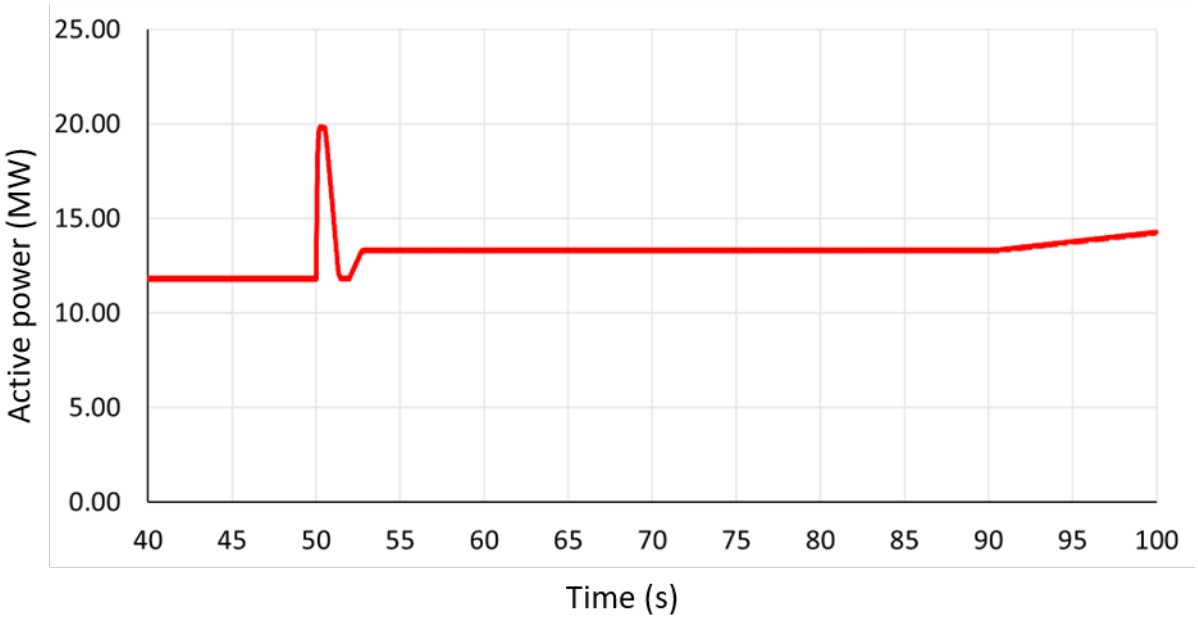

(c) Active power from the synchronous generator

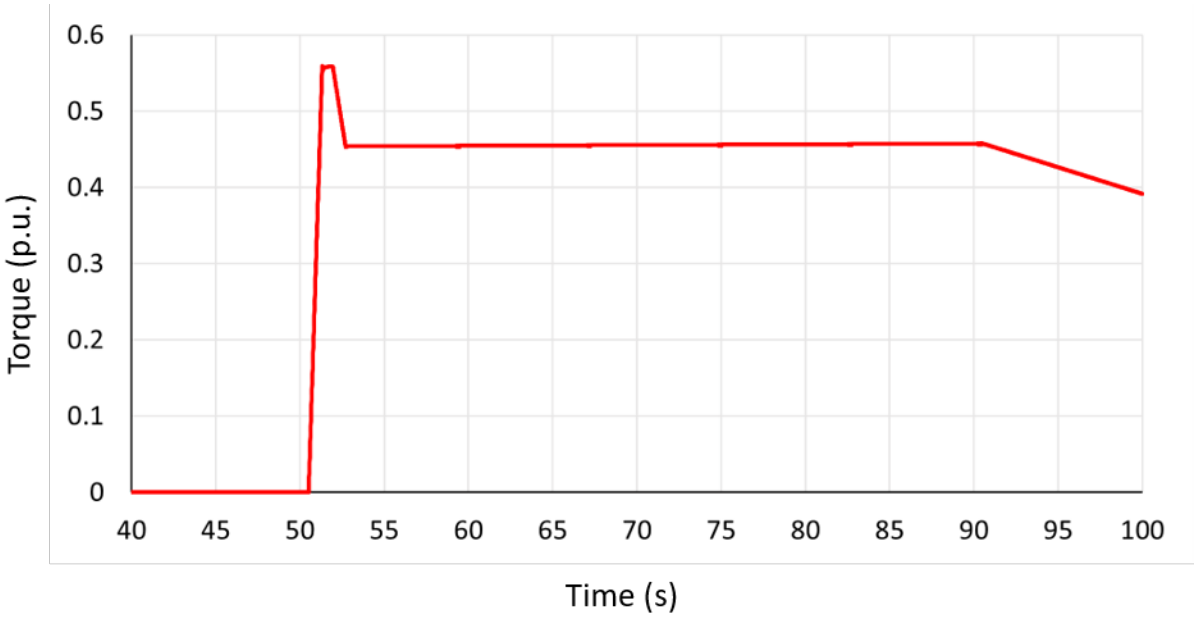

(d) Mechanical torque of the flywheel

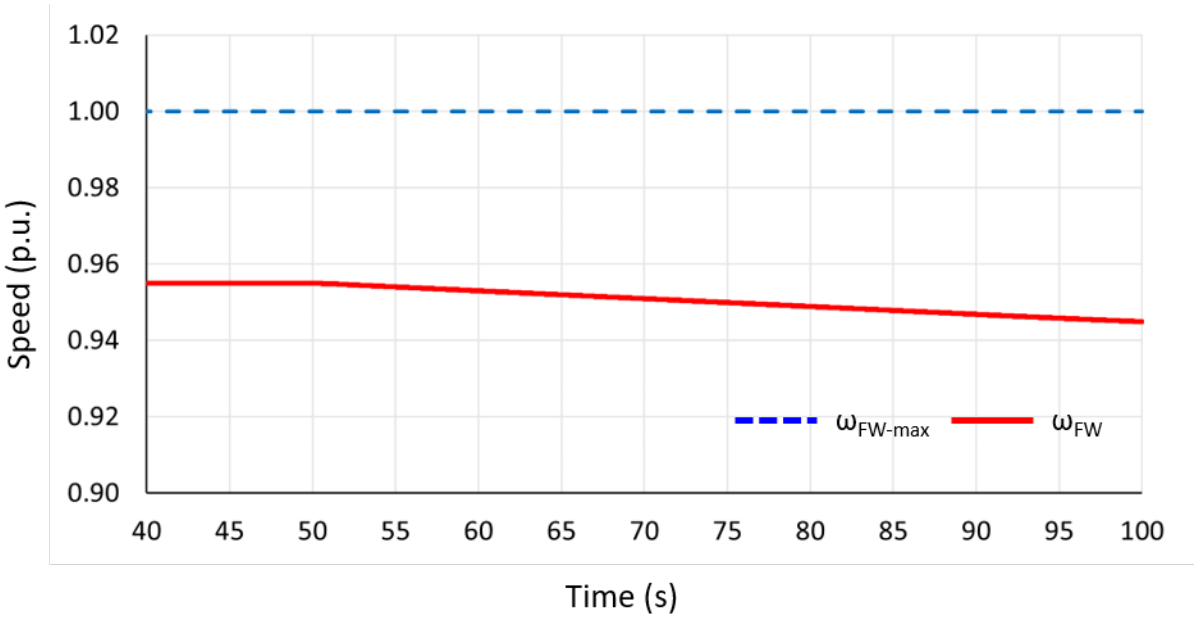

(e) Rotational speed of the flywheel
Figure 16: Result from case 4

4.6 Summary of cases

Table 4 shows the lowest frequency of the grid and when they occur. In each of the cases, the frequency is arrested at a higher value and closer to the tripping time with the proposed control scheme. Figure 17 (a) shows each case with the proposed control scheme, and figure 17 (b) shows each case with the traditional control method. It can be seen that the proposed control scheme shape is the same in all cases except for case two. This is due to the size of the PV being tripped off of the grid. Since the frequency droop is slower than in the previous cases, the frequency does not activate the control scheme until it is below 59.9 Hz, while the traditional control method continuously attempts to correct the frequency.

Table 4: Frequency nadir data

Case	With flywheel		Without Flywheel	
	Time (s)	Frequency (Hz)	Time (s)	Frequency (Hz)
5 MW	1.29	59.85829	3.77	59.67488
10 MW	1.33	59.75599	3.80	59.37025
2 MW	2.16	59.89654	3.74	59.87067
8 MW	1.28	59.79825	3.79	59.47983

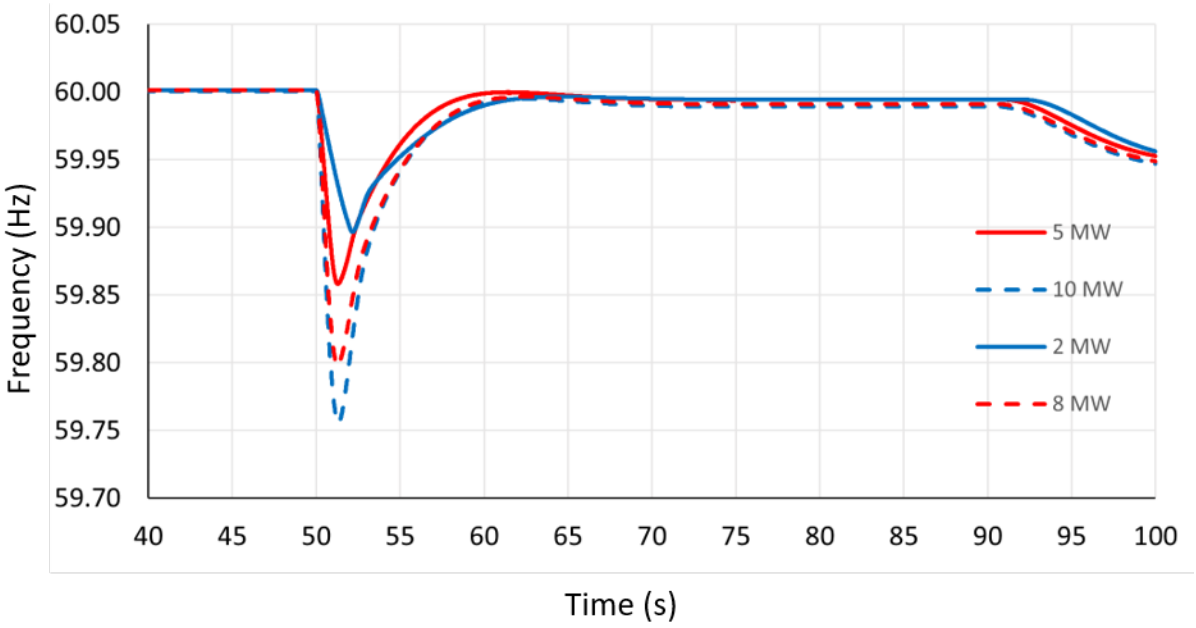

(a) System frequency with FESS

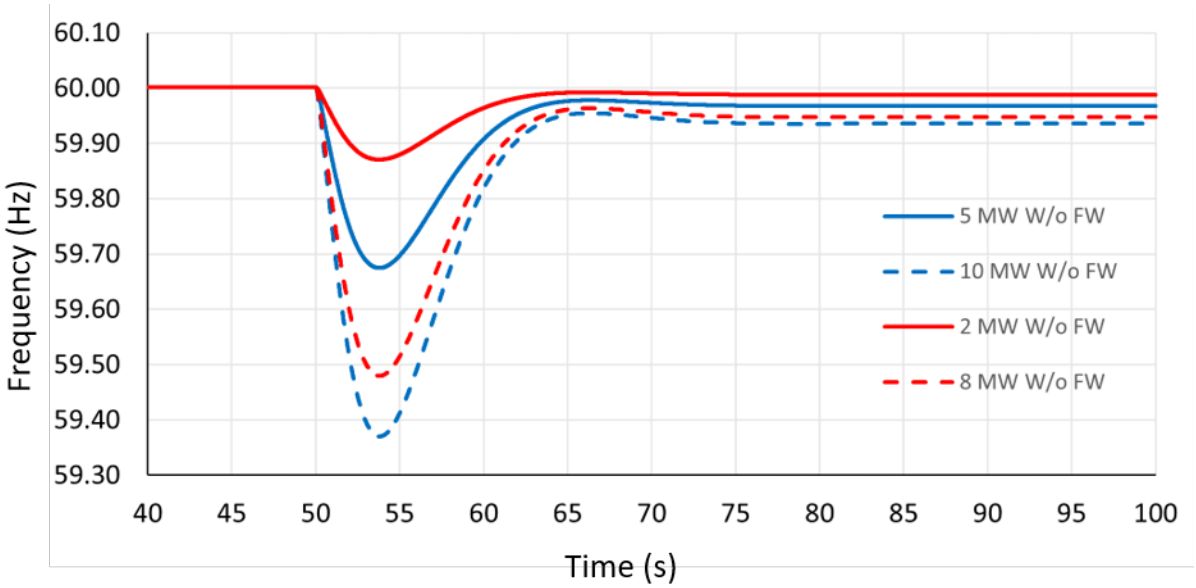

(b) System frequency without FESS

Figure 17: Summary of all cases

5. Conclusion and Future Work

5.1 Conclusion

Through the next decade, renewable energy generation will continue to be installed on power systems around the globe. As renewables that exhibit power intermittency make up larger percentages of the overall power supply, grid stability will become an issue. For ISOs to ensure stable operation of the grid, frequency and voltage must be maintained within acceptable levels. While many solutions for energy storage exist, FESSs are flexible in providing fast responses of both real and reactive power to the power system. Thus, this application can easily mimic the frequency responses of synchronous machines, such as the inertial response and frequency droop control. It may even be superior to synchronous machines in this application. It has been shown, that while the traditional method can achieve droop control, they are slow to correct the issue. This leads to large drops in the grid frequency, slowing down machines on the grid. The proposed control scheme is shown to arrest the frequency droop at higher levels and return the frequency to its nominal operating range without causing frequency swells. Therefore, it can provide rapid and accurate short-term frequency support for a sudden loss of generation or rapid changes in output. Thus, the results of the proposed scheme indicate it can cope with a wider range of short frequency events.

5.2 Future Work

While the proposed control scheme has shown promise for addressing frequency dips in the cases presented, more case studies should be conducted on larger systems to confirm the finding of this thesis. With more studies, the control method can be strengthened to better address the intermittency of renewable energy resources, like PV or wind. Since only PV was studied in the presented system, further work should be done with wind generation and with

mixes of other sources to model the dynamics of the power system more accurately. The focus of this work has been on frequency support, however, FESS is capable of both active and reactive power delivery. Therefore, a similar control scheme can be recreated to address other power system stability concerns, like voltage stability and angle stability.

References

[1] Ren21, “Renewables 2018 Global status report”, Ren21, Paris, France, 2018 [online], https://www.ren21.net/wp-content/uploads/2019/08/Full-Report-2018.pdf

[2] P. Kundur et al., "Definition and classification of power system stability IEEE/CIGRE joint task force on stability terms and definitions," in IEEE Transactions on Power Systems, vol. 19, no. 3, pp. 1387-1401, Aug. 2004,

[3] J. P. Barton and D. G. Infield, “Energy Storage and Its Use With Intermittent Renewable Energy,” *IEEE Trans. Energy Convers.*, vol. 19, no. 2, pp. 441–448, June 2004

[4] U. Datta et al, “Primary frequency control of a microgrid with integrated dynamic sectional droop and fuzzy based pitch angle control,” in International Journal of Electrical Power & Energy systems, Vol. 111, pp248-259, Oct. 2019

[5] ‘Beacon Power 400 Performance Specifications’, http://beaconpower.com/wp-content/themes/beaconpower/inc/beaconpower_40_ds_081414.pdf

[6] Beacon power, “20 MW Flywheel Energy Storage plant” , Sandia National Laboratories Energy storage systems program, 2014, https://www.sandia.gov/ess-ssl/docs/pr_conferences/2014/Thursday/Session7/02_Areseneaux_Jim_20MW_Flywheel_Energy_Storage_Plant_140918.pdf

[7] J. Ekanayake and N. Jenkins, “Comparison of the response of doubly fed and fixed-speed induction generator wind turbines to changes in network frequency,” *IEEE Trans. Energy Convers.*, vol. 19, no. 4, pp. 800–802, Dec. 2004.

[8] J. Morren, J. Pierik, and S. W. H. de Haan, “Inertial response of variable speed wind turbines,” *Electr. Power Syst. Res.*, vol. 76, no. 11, pp. 980–987, Jul. 2006.

[9] J. Morren, S. Haan, W. L. Kling, and J. A. Ferreira, “Wind turbines emulating inertia and supporting primary frequency control,” *IEEE Trans. Power Syst.*, vol. 21, no. 1, pp. 433–434, Feb. 2006.

[10] P. K. Keung, P. Li, H. Banakar, and B. T. Ooi, “Kinetic Energy of Wind-Turbine Generators System Frequency Support,” *IEEE Trans. Power Syst.*, vol. 24, no. 1, pp. 279–287, Feb. 2009.

[11] M. Kayikci and J. V. Milanovic, “Dynamic Contribution of DFIG-Based Wind Plants to System Frequency Disturbances,” *IEEE Trans. Power Syst.*, vol. 24, no. 2, pp. 859–867, May 2009.

[12] J. M. Mauricio, A. Marano, A. Gomez-Exposito, and J. L. Martinez Ramos, “Frequency Regulation Contribution Through Variable-Speed Wind Energy Conversion Systems,” *IEEE Trans. Power Syst.*, vol. 24, no. 1, pp. 173–180, Feb. 2009.

[13] I. D. Margaris, S. A. Papathanassiou, N. D. Hatziargyriou, A. D. Hansen, and P. Sørensen, “Frequency control in autonomous power systems with high wind power penetration,” *IEEE Trans. Sustain. Energy*, vol. 3, no. 2, pp. 189–199, Apr. 2012.

[14] J. Lee, E. Muljadi, P. Sørensen, and Y. C. Kang, “Releasable Kinetic Energy-Based Inertial Control of a DFIG Wind Power Plant,” *IEEE Trans. Sustain. Energy*, vol. 7, no. 1, pp. 279–288, Jan. 2016.

[15] J. Lee, G. Jang, E. Muljadi, F. Blaabjerg, Z. Chen, Y. C. Kang, “Stable Short-Term Frequency Support Using Adaptive Gains for a DFIG-Based Wind Power Plant,” *IEEE Trans. Energy Convers.*, vol. 31, no. 3, pp. 1068–1079, Sept. 2016.

[16] M. Hwang, E. Muljadi, J. W. Park, P. Sørensen, and Y. C. Kang, “Dynamic Droop-Based Inertial Control of a Doubly-Fed Induction Generator,” *IEEE Trans. Sustain. Energy*, vol. 7, no. 3, pp. 924–933, Jul. 2016.

[17] M. Hwang, E. Muljadi, G. Jang, and Y. C. Kang, "Disturbance-Adaptive Short-Term Frequency Support of a DFIG Associated With the Variable Gain Based on the ROCOF and Rotor Speed," *IEEE Trans. Power Syst.*, vol. 32, no. 3, pp. 1873–1881, May 2017.

[18] N. R. Ullah, T. Thiringer, and D. Karlsson, "Temporary Primary Frequency Control Support by Variable Speed Wind Turbines—Potential and Applications," *IEEE Trans. Power Syst.*, vol. 23, no. 2, pp. 601–612, May 2008.

[19] S. E. Itani, U. D. Annakkage, and G. Joos, "Short-Term Frequency Support Utilizing Inertial Response of DFIG Wind Turbines," *2011 IEEE Power and Energy Society General Meeting*, Detroit, MI, USA, 24–28 July 2011.

[20] M. Kang, K. Kim, E. Muljadi, J. W. Park, and Y. C. Kang, "Frequency Control Support of a Doubly-Fed Induction Generator Based on the Torque Limit," *IEEE Trans. Power Syst.*, pp. 4575–4583, Nov. 2016.

[21] D. Yang, J. Kim, Y. C. Kang, E. Muljadi, N. Zhang, J. Hong, S. H. Song, and T. Zheng, "Temporary Frequency Support of a DFIG for High Wind Power Penetration," *IEEE Trans. Power Syst.*, vol. 33, no. 3, pp. 3428–3437, May 2018.

[22] FACT SHEET Frequency Regulation and Flywheels' https://web.archive.org/web/20100331042630/http://www.beaconpower.com/files/Flywheel_FR-Fact-Sheet.pdf

[23] E. Muljadi and V. Gevorgian, "Flywheel Energy Storage—Dynamic Modeling," *2017 Ninth Annual IEEE Green Technologies Conference*, Denver, CO, USA, Mar. 2017.

[24] J. Machowski, J. W. Bialek, and J. R. Bumby, "Frequency stability and control," in *Power System Dynamics: Stability and Control*, 2nd ed. Wiltshire, U.K.: Wiley, 2008.

[25] C. Concordia, L. H. Fink, and G. Poullikkas, "Load shedding on an isolated system," *IEEE Trans. Power Syst*., vol. 10, no. 3, pp. 1467–1472, Aug. 1995.

[26] R. Cardenas, R. Pena, G. Asher, and J. Clare, "Control Strategies for Enhanced Power Smoothing in Wind Energy Systems Using a Flywheel Driven by a Vector-Controlled Induction Machine," *IEEE Trans. Ind. Electron.*, vol. 48, no. 3, pp. 625–635, June 2001.

[27] R. Cardenas, R. Pena, G. Asher, J. Clare, and R. Blasco-Gimenez, "Control Strategies for Power Smoothing Using a Flywheel Driven by a Sensorless Vector-Controlled Induction Machine Operating in a Wind Speed Range," *IEEE Trans. Ind. Electron.*, vol. 51, no. 3, pp. 603–614, June 2004.